



UNIVERSITY OF TRENTO

International PhD Program in Biomolecular Sciences

XXX Cycle

**Characterization of Retinal Defects in *Engrailed-2*
Knockout (*En2*^{-/-}) Mice, a Model for Autism Spectrum
Disorders (ASD)**

Centre for Integrative Biology (CIBIO), University of Trento

PhD Thesis of Xuwen Zhang

Tutor

Simona Casarosa, Ph.D.

Centre for Integrative Biology (CIBIO), University of Trento

CNR Neuroscience Institute, National Research Council (CNR), Pisa

Advisor

Andrea Messina, Ph.D.

Centre for Mind/Brain Sciences (CIMEC), University of Trento

Academic Year 2016-2017

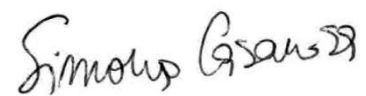
Declaration

I Xuwen Zhang confirm that this is my own work and the use of all material from other sources has been properly and fully acknowledged.

Signature of the PhD candidate

A handwritten signature in black ink that reads "Xuwen Zhang". The signature is written in a cursive style with a large, sweeping flourish at the end of the last name.

Signature of the Tutor

A handwritten signature in black ink that reads "Simon Gassner". The signature is written in a cursive style with a large, sweeping flourish at the end of the last name.

INDEX

LIST OF ABBREVIATIONS.....	4
ABSTRACT.....	6
1. INTRODUCTION.....	8
1.1 Autism Spectrum Disorders.....	8
1.1.1 Genetics of autism.....	11
1.1.2 Neuropathological findings in autism.....	13
1.2 Animal Models of Autism Spectrum Disorders.....	15
1.2.1 Mutant Mouse Models.....	15
1.2.2 Other Animal Models.....	18
1.3 <i>Engrailed 2</i> Knock-out Mice.....	19
1.3.1 <i>Engrailed 2</i> gene.....	19
1.3.2 <i>Engrailed 2</i> knock-out (<i>En2^{-/-}</i>) mice.....	22
1.4 Mammalian Visual System.....	25
1.4.1 Retinal development in mammals.....	26
1.4.2 Retinal structure.....	28
1.5 Sensory Processing in Autism.....	31
2. AIM OF THE THESIS.....	33
3. MATERIALS AND METHODS.....	35
3.1 Animals.....	35
3.2 Laser Capture Microdissection (LCM).....	36
3.3 In Situ Hybridization (ISH).....	37
3.4 RNA Extraction and Quantitative RT- PCR (RT- qPCR).....	39
3.5.1 Immunohistochemistry on Retinal Sections	40
3.5.2 Whole Mount Immunohistochemistry	40
3.6 Image Acquisition and Cell Counting.....	42

3.7 Protein Extraction and Western Blotting.....	43
3.8 Statistical Analysis.....	45
4. RESULTS.....	46
4.1 <i>En2</i> expression in adult wild-type mice retina.....	46
4.2 Reduction of rhodopsin expression in <i>En2</i> ^{-/-} adult mouse retina.....	48
4.3 Decreased expression of S-opsin mRNA in <i>En2</i> ^{-/-} adult retina.....	51
4.4 Reduced pcp2 expression in bipolar cells in <i>En2</i> ^{-/-} adult mice.....	54
4.5 Decreased Calbindin+ horizontal cells density in <i>En2</i> ^{-/-} adult retina.....	57
4.6 Retinal amacrine cells characterization in <i>En2</i> ^{-/-} mice.....	60
4.7 Density of Brn-3a+ retinal ganglion cells in <i>En2</i> ^{-/-} mice.....	63
4.8 Reduced b-wave in ERGs of <i>En2</i> ^{-/-} mice under scotopic conditions.....	65
5. DISCUSSION.....	69
6. CONCLUSIONS AND FUTURE PERSPECTIVES.....	76
REFERENCES.....	79
ACKNOWLEDGMENTS.....	96

LIST OF ABBREVIATIONS

ASD: Autism Spectrum Disorder

En2: Engrailed 2

ONL: Outer nuclear layer

INL: Inner nuclear layer

GCL: Ganglion cells layer

OPL: Outer plexiform layer

IPL: Inner plexiform layer

S opsin: Short wavelength sensitive opsin

M opsin: Middle wavelength sensitive opsin

PKC α : Protein kinase C, alpha

PSD95: Post-synaptic density protein 95

Pcp2: Purkinje cell protein 2

CB: Calbindin

HC: Horizontal cells

AC: Amacrine cells

GC: Ganglion cells

Brn-3a: Brain-specific homeobox/POU domain protein 3a

Rho: Rhodopsin

GAPDH: Glyceraldehyde 3-phosphate dehydrogenase

PV: Parvalbumin

P10: Postnatal 10 days

P30: Postnatal 30 days

ERG: Electroretinogram

ABSTRACT

Mice lacking the homeobox-containing transcription factor *En2* (*En2*^{-/-} mice) are considered as a reliable animal model for investigating the neurodevelopmental basis of autism spectrum disorders, as they display some ASD-related anatomical deficits, including cerebellar hypoplasia (Joyner A L, et al., 1991), reduced Purkinje neurons numbers (Kuemerle B, et al., 1997), altered anatomy of the amygdala (Kuemerle B, et al., 2007), and a significant loss of forebrain GABAergic interneurons (Sgadò P et al., 2013). *En2*^{-/-} mice also display autistic-like behavioral defects, including decreased sociability (Brielmaier J, et al., 2012), enhanced seizure susceptibility (Tripathi P P, et al., 2009) and impaired spatial learning and memory (Provenzano G, et al., 2014) (Cheh M A, et al., 2006). A recently published study from our laboratory revealed that *En2*^{-/-} mice displayed an altered disposition of GABAergic circuits in the visual cortex, that might contribute to alter binocularity and plasticity of the visual system, while leaving other visual functional properties (acuity, response latency, receptive field size) unaffected (Allegra M, et al., 2014). Moreover, preliminary experiments performed in our laboratory suggested that, at cellular level, the retina of *En2*^{-/-} mice showed alterations in the number of specific cell subtypes compared with the retina of WT littermates. More importantly, an increasing number of studies published in the past years indicated that difficulties in sensory processing might somehow contribute to

the pathogenesis of autism (*Robertson C E, Simon B C, 2017*). Therefore, we decided to investigate the possible retinal defects in the *En2*^{-/-} mice. We showed for the first time that the *En2* gene is expressed in all nuclear layers of the adult mouse retina. We also found that *En2*^{-/-} adult mice showed a significantly decreased number of Calbindin (Calbindin⁺) positive horizontal cells, and a significantly increased number of Calbindin⁺ amacrine/ganglion cells. The number of Brn-3a (Brn-3a⁺) positive ganglion cells displayed no difference with respect to wild-type littermates. In addition, *En2*^{-/-} adult mice showed a significantly reduced expression of the rod photoreceptor marker rhodopsin at both mRNA and protein levels, and a significant reduction of the S-cone photoreceptor S opsin, the bipolar cells marker pcp2, and the GABAergic interneurons marker parvalbumin. Electroretinogram (ERG) analysis revealed that the amplitude of b-wave in *En2*^{-/-} mice scotopic ERG was significantly reduced as compared with controls. Together, all these data indicate that *En2*^{-/-} mice exhibit retinal defects at molecular, cellular and functional level, whose significance needs to be further investigated.

1. INTRODUCTION

1.1 Autism Spectrum Disorders

Autism spectrum disorders (ASD) encompasses a cluster of highly heterogeneous neurodevelopmental disorders defined by a triad of core behavioral abnormalities: the inability to engage in reciprocal social interactions, deficits in language and communication, and restricted interests accompanied by repetitive behaviors (*Banerjee S, et al 2014*) (*Abrahams B S, Geschwind D H, 2008*) (*Betancur C, et al., 2009*) (*Levitt P, Campbell D B., 2009*) (*Peça J, et al., 2011b*) (*Zoghbi H Y, Bear M F, 2012*). According to the new edition of the Diagnostic and Statistical Manual of Mental Disorders (DSM-V; 2013), a guide created by the American Psychiatric Association used to diagnose mental disorders, ASD encompasses narrowly defined autism, social disintegration disorder, Asperger's disorder, and pervasive developmental disorder not otherwise specified (PDD-NOS).

Autism spectrum disorder has an impact on early brain development. Obvious signs and symptoms appear within the first 3 years of life and persist into adulthood (*Banerjee S, et al., 2014*). Recent studies demonstrate that the prevalence of ASD has been steadily rising, accompanied by widespread speculations concerning the factors that might be responsible. During the years 1970 to 1980, the prevalence of autism was estimated at around 0.05%

(*Wing L, et al., 1976*) (*Ritvo E R, et al., 1989*), while recently published epidemiological studies reveal an estimated prevalence of more than 1% of the world's population were affected by ASD (*Elsabbagh M, et al., 2012*) (*Baio J, et al., 2014*), and the incidence of ASD among 8-year-old children across 11 sites in United States is now estimated at 11.3 per 1000 (1 in 88) (*Baio J, et al., 2014*). Moreover, ASD exhibits a gender bias, as it affects more males than females; particularly in the individuals with a normal intelligence (more than 5 males/1 female affected) (*Bourgeron T, 2015*) (*Miles J H, et al., 2005*).

ASD was first described by Kanner, who assumed autism was a kind of inborn disturbance, though he also questioned if environmental factors could contribute to it (*Kanner L, 1943*). This hypothesis has been supported by many studies indicating how environmental factors also likely contribute to some autistic cases, though they still need to be further investigated (*Newschaffer C J, et al., 2007*). A prominent example is the prenatal exposure to agents such as valproic acid. A study on the effect of prenatal exposure to valproate revealed that, when the mother was exposed to valproate during pregnancy, children had a higher risk of ASD and childhood autism compared with children born from women who did not use valproate or stopped the intake of valproate during the pregnancy. This suggests that maternal use of valproate during pregnancy could contribute to a significantly increased risk of autism spectrum disorder and childhood autism in the offspring (*Christensen J. et al., 2013*). Environmental factors are not the only determinants that contribute to the

pathology of ASD, and likely exert their effect via complex genetic interactions. For instance, patients who have phenylketonuria are more likely to develop ASD and other manifestations of the disease if they are on a diet consuming more phenylalanine (Manzi B, et al., 2008). This kind of interactions can also be observed in other metabolic types of ASD caused by mutations in *BCKDK* (*Branched Chain Ketoacid Dehydrogenase Kinase*). Specifically, *BCKDK* mutations were identified in core families with autism, epilepsy and intellectual disability (ID) (Novarino G., 2012). *BCKDK* encoded protein contributes to inactivating the E1-alpha subunit of branched chain ketoacid dehydrogenase (BCKDH). *Bckdk* knockout mice showed abnormal brain aminoacid profiles and autistic behavioral deficits, and these defects could be treated with high consumption of branched-chain amino acids (Novarino G., 2012).

Numerous findings published in the past decades confirmed the effects of genetic factors that could be the key component of ASD. Studies on twins and some case reports revealed an average monozygous twin concordance of 64% and an average dizygous twin concordance of 9%, compared to a population prevalence estimated to be 0.05% at the time of the study (Smalley S L, et al., 1980), strongly suggesting the high heritability of autism. Meanwhile, there is increasing evidence from Mendelian diseases linked with ASD indicating that mutations in single genes can greatly increase the risk for ASD. These include mutations in genes such as *FMR1* (Fragile X syndrome), *TSC1/TSC2* (Tuberous sclerosis complex), *CACNA1C* (Timothy syndrome),

and many other single genes, which are supposed to account for 10-20% of total ASD cases (*Berg J M, et al., 2012*) (*Abrahams B S, et al., 2008*). While the increasing evidence shows that both genetic and environmental factors can contribute to ASD, the relative importance of genetic versus environmental factors in the etiology of ASD is still a matter under debate.

1.1.1 Genetics of autism

Autism spectrum disorders are a type of common and heritable neuropsychiatric disorders. Genetically, autism can be generally classified into two forms: syndromic and nonsyndromic (*Miles J H, 2011*) (*Schaaf C P, 2011*) (*Singh S K, Eroglu C, 2013*). Syndromic ASD is a type of ASD with known genetic cause and unique clinical symptoms, which represent only a few total ASD cases, while non-syndromic ASD typically has unknown genetic causes, and accounts for the major percentage of total ASD cases (*Sztainberg Y, Zoghbi H Y, 2016*). Autism for which genetic causes are known can be further classified in: cytogenetically visible chromosomal abnormalities (~5%), copy number variants (CNVs) (i.e., variations in the number of copies of one segment of DNA, including deletions and duplications) (10-20%), and single-gene disorders (~5%) (*Miles J H, 2011*) (*Rosti R O, et al., 2014*) (*Robert C, et al., 2017*). Visible cytogenetic abnormalities were found with the help of high-resolution karyotype analysis in approximately 5% of children with ASD, and another 3–5% of ASD cases were identified with the assistance of

fluorescence in situ hybridization (FISH) techniques (*Miles JH, 2011*). Cytogenetic abnormalities were found on almost every chromosome, though only a few which occur with a high frequency can be located to a specific autism gene (*Reddy K S, 2005*) (*Vorstman J A, 2006*) (*Lintas C, Persico A M, 2009*). Copy number variations (CNVs) exist in the genome where sections of the genome are repeated and the number of repeats in the genome are different in different species (*McCarroll SA, et al., 2007*). The number of genetic ASD cases which involve CNVs has increased with the assistance of array Comparative Genomic Hybridization (aCGH) (*Robert C, et al., 2017*), a technique used to evaluate the DNA copy number alterations associated with chromosome abnormalities in high-resolution (*Bejjani B A, Shaffer L G, 2006*). Some ASD cases are caused by single genes mutations, such as NF1 (Neurofibromatosis), UBE3A (Angelman syndrome), SHANK3, and PTEN (*Berkel S, et al., 2010*) (*Durand C M, et al., 2007*) (*Geschwind D H, Levitt P, 2007*) (*Hatton D D, et al., 2006*) (*Veenstra-Vanderweele J, et al., 2004*). Meanwhile, genome-wide association studies (GWAS) indicated that DLX, Reelin, and Engrailed genes are also linked to autism (*Gadad B S, et al., 2013*).

Angelman syndrome (AS) shares some common behavioral phenotypes with autism. There are differences in severity of autistic features across subtypes of AS, with some behavioral features being unique to AS and some representing all forms of developmental disability (*Bonati M T, et al., 2007*). AS is a

neurodevelopmental disorder caused by mutations in the ubiquitin-protein ligase E3A gene (UBE3A) that can be ascribed to a variety of genetic abnormalities of the imprinted 15q11-q13 chromosomal region (*Horsthemke B, Buiting K, 2006*). This syndrome is caused by different types of genetic alterations: deletion on the maternal chromosome 15 (70%), paternal chromosome 15 uniparental disomy (UPD; 2%), point mutations of the UBE3A gene (10%) and epimutations. No identifiable molecular abnormality is found in the remaining AS patients (10-13%) (*Bonati M T, et al., 2007*). UBE3A mutations caused by the loss of the E6-associated protein carboxyl terminus domain were considered to be linked to ASD (*Bonati M T, et al., 2007*).

In addition, Fragile X Syndrome (FXS) is another common single gene mutation disorder which is associated with ASD. FXS is caused by the expansion of the CGG trinucleotide repeats in the 5' untranslated region of the FMR1 gene (*Miles J H, 2011*). The *FMR1* gene encodes for fragile X mental retardation protein (FMRP) (*De Rubeis S, et al., 2012*), a type of RNA-binding protein responsible for post-transcriptional regulation. Estimated 50% of FXS could also be diagnosed as autism based on symptoms and phenotype, although different studies may be variable (*Abbeduto L, et al., 2014*).

1.1.2 Neuropathological findings in autism

ASD symptoms are due to neuropathological changes in different brain

regions, even if there is yet no consensus regarding all brain regions affected by the disease. Autistic patients post-mortem analysis revealed an abnormal brain growth, and the areas which are considered to be involved in the development of social, communication and motor abilities displayed white matter abnormalities (*Baribeau D A, Anagnostou E A, 2013*) (*Mostofsky S H, et al., 2009*). Specifically, autistic brains demonstrated an overgrowth in the region of the frontal lobe, cerebellum, and limbic structures, and a volume loss in the area of corpus callosum and cingulum (*Baribeau D A, Anagnostou E A, 2013*). Meanwhile, both cerebellar gray and white matters regions also displayed a decreased volume (*Baribeau D A, Anagnostou E A, 2013*).

Autism involves many different pathological abnormalities, including alterations in the development of neurons in the forebrain limbic system, a decrease in the cerebellar Purkinje cell population and age-related changes in neuronal size and number in some cerebellar nuclei and in the inferior olive (*Kemper T L, Bauman M, 1998*) (*Romero-Munguía M Á, 2011*). Loss of Purkinje neurons is considered to be related to GABA neurotransmission dysfunction. Abnormal GABA release in Purkinje cells and Purkinje cells alterations could be further related to the increased expression level of GAD67 mRNA in cerebellar interneurons of ASD patients (*Yip J, et al., 2008*). The above-mentioned abnormalities could have a severe impact on many developmental processes, including neuronal migration, axodendritic outgrowth, synaptogenesis, and pruning (*DiCicco-Bloom E, 2006*). These results suggest that delayed neuronal

maturation could contribute to the pathogenesis of autism (*Minshew N J, Williams D L, 2007*). An increased volume of the amygdala was frequently observed in anatomical studies of autistic children brains. The deficits in amygdala could be associated with the social communication deficits and increased anxiety of autistic patients (*Haznedar M M, et al., 2000*). Neuropathological studies in the limbic system of autism mouse models unveiled several abnormalities in the hippocampus, amygdala, and other limbic structures: decreased neuronal size, increased neuronal packing density, and decreased complexity of dendritic arbors (*Schmahmann J D, et al., 2009*) (*Gadad B S, et al., 2013*). Together, convergent evidence from different studies suggests that anatomical defects in the amygdala and cortical region could be contributing to the deficits in dendritic spine reorganization and consolidation (*Gadad B S, et al., 2013*). Furthermore, abnormal spine generation or deficits in spine reorganization, elimination, and pruning are anatomical traits which are associated with the pathology of autism (*Hutsler J J, Zhang H, 2010*).

1.2 Animal Models of Autism Spectrum Disorders

1.2.1 Mutant Mouse Models

In order to better understand molecular mechanisms and anatomical/functional defects in ASD, laboratory rodents are widely used for autism research. The use of these models is based on the following advantages: well-characterized

behaviors; many well-established behavioral methods and techniques to study nervous system; accessible to chemical agents or genetic interventions tests; susceptible to social behavior alterations due to their nature of social animals (Cryan J F, Holmes A, 2005). The generation of mouse models for ASD by targeted deletion of ASD-associated genes has become an increasingly important and essential tool to investigate the neurodevelopmental basis of ASD, as well as the molecular, cellular, anatomical, electrophysiological and behavioral consequences of gene dysfunctions in ASD (Provenzano G, et al., 2012). ASD-associated genes present in SFARI (Simons Foundation Autism Research Initiative) database can be roughly classified into three groups: syndromic ASD genes, strong candidate genes and genes with suggestive or minimal evidence of ASD association (Provenzano G, et al., 2012). Mutant mice generated by specifically deleting syndromic ASD genes, such as CNTNAP2, FMR1, NF1, PTEN, SHANK3, TSC1/2, and UBE3A, display autistic symptoms in the context of other neurological disorders with symptoms caused by the specifically targeted gene (Provenzano G, et al., 2012). For example, *Fmr1* KO mice demonstrated complex behavioral phenotypes, including some ASD-like symptoms, such as attention dysfunction (Moon J, et al., 2006) and seizures (Yabut O, et al., 2007).

Strong ASD candidate genes, including CNTN4 and NRXN1, are a group of genes which are validated in many different independent studies showing their strong link to ASD (Provenzano G, et al., 2012). Contactin4 (CNTN4), a

contactin family axonal cell adhesion molecule, plays an essential role in the formation of axonal connections in different brain regions (cerebellum, thalamus, amygdala, and cerebral cortex) during development (*Fernandez T, et al., 2004*). *Cntn4*^{-/-} mice displayed aberrant projections of olfactory sensory neurons to multiple glomeruli, suggesting that *Cntn4*^{-/-} mice have olfactory processing deficits, which is also considered as ASD-related symptom (*Bennetto L, et al., 2007*) (*Brewer W J, et al., 1996*).

Genes with suggestive or minimal evidence of ASD association genes are a class of candidate genes, which are validated in few independently replicated studies, including EN2, FOXP2, GABRB3, NGLNs, OXT/OXTR and RELN (*Provenzano G, et al., 2012*). Mice lacking these genes could model some phenotypes of ASD. For instance, the RELN gene encodes the extracellular matrix glycoprotein Reelin, which plays a role in neuronal migration and lamination of the cerebral cortex during embryogenesis. Mice lacking Reelin (*reeler* mice) show some ASD-related defects: decreased number of GAD67-positive cortical neurons (*Liu W S, et al., 2001*), decreased GABA turnover (*Carboni G, et al., 2004*) and improper layer positioning of GABAergic interneurons in the mature cerebral cortex (*Yabut O, et al., 2007*). Other studies also reported some ASD-like behaviors in these mice (*Macri S, et al., 2010*).

1.2.2 Other Animal Models

In addition to mouse models, monkeys, songbirds, and zebrafish are also used in modeling autistic symptoms and molecular mechanisms (*Hrabovska S V, Salyha Y T, 2016*) (*Meshalkina D A, 2017*). Rhesus monkeys were used as a model to evaluate the effects of the neonatal amygdala or hippocampus damage on the emergence of stereotypies, that was supposed to be related to the neurobiological basis of repetitive stereotypes in neurodevelopmental disorders, such as autism (*Bauman M D. et al., 2008*). Songbirds were used as an animal model to dissect the genetic bases of ASD (*Panaitof S C, 2012*). Recently, zebrafish is becoming a rapidly emerging animal model for understanding the pathogenesis of complex psychiatric disorders, including autism and discovering new therapeutic approaches (*McCammon J M, Sive H, 2015*) (*Levitas-Djerbi T, Appelbaum L, 2017*) (*Meshalkina D A, 2017*). Compared with other animal models for autism, zebrafish have many advantages for investigating the pathogenesis of ASD, including low-cost, rapid transient genetic assays, available for live imaging experiments, accessibility of whole brain with the use of optogenetic tools for deciphering neural circuits and their function, and amenability to chemical screens to define potential therapies (*McCammon J M, Sive H, 2015*) (*Kalueff A V, et al., 2013*). To be specific, zebrafish can be used to model ASD-like social phenotypes (such as social preference and repetitive behaviors) and be also used as genetic models relevant to ASD (*Levitas-Djerbi T, Appelbaum L, 2017*). For example, a recent study showed zebrafish larvae displayed autism-like

behavioral deficits, such as increased cycle swimming and edge preference, following maternal exposure to the mixture of the water soluble fraction of crude oil and lead (Pb) (Wang Y, et al., 2016).

1.3 *Engrailed 2* Knock-out Mice

1.3.1 *Engrailed 2* gene

Engrailed 2 is a homeodomain-containing transcription factor. The gene *Engrailed* was initially identified in *Drosophila*, required for the establishment of anterior-posterior compartments in each segment of the body (Morata G, Lawrence P A, 1975). From then on, *Engrailed* homologues were also discovered in different types of organisms (Gibert J M, 2002). Vertebrate homologs were identified in chick (Gardner C A, et al., 1988), mice (Joyner A L, et al., 1985), frogs (Hemmati-Brivanlou A, et al., 1991), fish (Fjose A, et al., 1988), and human (Poole S J, et al., 1989). Generally, there are 2-3 *Engrailed* genes in vertebrates, which in most species play a role in conferring specific identity to defined areas and neurons (Wizenmann A, et al., 2015).

In mouse, there are two *Engrailed* genes: *En1* and *En2*, that share more than 90% of homology at the protein level in the homeodomain region (Joyner A L, Martin G R, 1987). *Engrailed* proteins contain highly conserved homeodomains that confer their transcriptional regulation function (Logan C, et al., 1992) (Morgan R, 2006). The homeodomain is a sequence of about 60

amino acids that is conserved in all types of homeodomain proteins, and it is composed of three alpha-helices, of which the third binds double-stranded DNA (*Morgan R, 2006*). In addition to the homeodomain, Engrailed genes also have other four regions of similarity (EHs), EH1-EH3 and EH5 (Fig 1.3.1.1). EH1 and EH5 play a role in mediating transcriptional repression by recruiting the co-repressor *groucho* (*Tolkunova E N, et al., 1998*), while EH2 and EH3 bind PBX, a second homeodomain-containing transcription factor that modifies the DNA binding affinity and specificity of the En gene (*Peltenburg L T, Murre C, 1997*) (*Van Dijk M A, Murre C, 1994*). Apart from EHs, Engrailed proteins also have other properties: the ability to be secreted (*Joliot A, et al., 1998*), the ability to be internalized (*Cosgaya J M, et al., 1998*), and the ability to bind directly to the eukaryotic translation initiation factor 4E (eIF4E) by a sequence localized at the N-terminal (*Nédélec S, et al., 2004*).

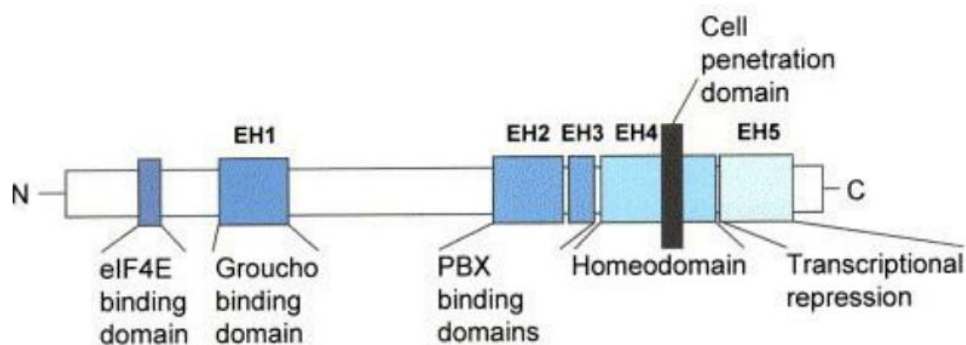


Fig 1.3.1.1 Functional domains of Engrailed proteins (*Morgan R, 2006*).

Genome-wide association study in humans revealed that two intronic single

nucleotide polymorphisms (SNP) in *EN2* gene, rs1861972 and rs1861973, showed a strong link with ASD (Jiyeon C, et al., 2011) (Benayed R, et al., 2005) (Gharani N, et al., 2004) (Benayed R. et al., 2009). Interestingly, later studies revealed that one SNPs (rs1861973, A-C haplotype) in *EN2* gene is functional, suggesting *EN2* as a possible ASD susceptibility gene and the A-C haplotype as a possible risk allele (Benayed R, et al., 2009). Meanwhile, epigenetic changes in the *En2* promoter were observed in the cerebellum of some autistic individuals (James S J, et al., 2014). All these results suggest a link between the *En2* gene and autism.

Engrailed genes are also involved in the development of the vertebrate visual system. Early expression of Engrailed in the dorsal mesencephalon contributes to the development and organization of a visual structure, the optic tectum/superior colliculus (Wizenmann A, et al., 2015). Moreover, Engrailed also plays a role in regulating the expression of Ephrin, an axon guidance signaling molecule found in the tectum/superior colliculus (Brunet I. et al., 2005). In fact, Engrailed was reported to function as an axon guidance cue in synergy with the Ephrin system, and this is proposed to contribute to enhancing retinal topographic precision (Wizenmann A. et al., 2009).

1.3.2 Engrailed 2 knock-out (*En2*^{-/-}) mice

In mouse, the *En2* gene plays an important role in the regionalization,

patterning and neural differentiation of the midbrain and hindbrain regions during embryonic development (Cheng Y, et al., 2010) (Gherbassi D, Simon H H, 2010) (Herrup K, et al., 2005) (Joyner A L, 1996) (Orvis G D, et al., 2012) (Sgaier S K, et al., 2007). In addition, *En* genes also are involved in neural survival during developmental stages (Alvarez-Fischer D, et al., 2011). *En2* is widely expressed in the developing mouse mesencephalon (midbrain) and rhombomere 1 (including the cerebellum primordium), starting at the neural plate stage (embryonic day 8.5) and continuing throughout embryonic and postnatal development (Joyner A L, 1996) (Davis C A, Joyner A L, 1988) (Wilson S L, et al., 2011). More recent studies also showed that *En2* mRNA is also expressed in the hippocampus and cerebral cortex of adult mice (Tripathi P P, et al., 2009) (Sgadò P, et al., 2013).

Mice lacking the homeobox-containing transcription factor *En2* (*En2*^{-/-}) can be considered as a reliable animal model for investigating the neurodevelopmental basis of ASD. *En2*^{-/-} mice display some ASD-related anatomical deficits. They are viable and fertile and display a mild phenotype which includes a decreased size in cerebellar volume and abnormal foliation in the cerebellum (Joyner A L, et al., 1991). A later study demonstrated that *En2*^{-/-} mice displayed a decrease in cerebellar size, mild abnormalities in patterning foliation of cerebellum accompanied by the reduction of the Purkinje, granule, deep nuclear, and inferior olive neurons (Kuemerle B, et al., 1997). *En2*^{-/-} mice also displayed an obvious anterior shift in the position of the amygdala in the

cerebral cortex (*Kuemerle B. et al., 2007*). Our lab has shown that *En2*^{-/-} mice showed a significant reduction in the number of parvalbumin (PV), somatostatin (SOM) and neuropeptide Y (NPY) expressing GABAergic interneurons detected in the hippocampus and cerebral cortex of adult mice, suggesting that *En2* plays in an important role in the development and/or maintenance of selected populations of GABAergic interneurons of the mouse hippocampus and somatosensory cortex (*Sgadò P, et al., 2013*). This is in agreement with previous findings in other mouse models for ASD, which also displayed abnormalities in GABAergic neuron circuitry (*Sgadò P, et al., 2011*) (*Provenzano G, et al., 2012*). To be specific, ASD mice including *Fmrp*, *Neurologin 3* mutant mice, and also valproic acid-treated mice were shown to have a noticeable reduction of PV-expressing interneurons in the somatosensory cortex, which was also detected in *En2*^{-/-} mice (*Gogolla N, et al., 2009*).

In addition to anatomical deficits, *En2*^{-/-} mice also display some ASD-like behaviors. Behavioral studies on adult mice found that they displayed neurobehavioral deficits in social as well as learning and memory tasks (*Cheh M A, 2006*) (*Brielmaier J, et al., 2012*). In particular, they displayed very significant deficits in reciprocal social interactions both in juvenile and adults (*Brielmaier J, et al., 2012*). Besides, *En2*^{-/-} mice also displayed an increased susceptibility to seizures (*Tripathi P P, et al., 2009*), which was frequently clinically witnessed in autistic patients (*Gilby K L, O'Brien T J, 2013*). It is

noteworthy that *En2*^{-/-} adult mice displayed robust spatial learning and memory defects, detected by the Morris Water Maze test (MWM) (Cheh M A, 2006) (Briellmaier J, et al., 2012) (Provenzano G, et al., 2014a). Further investigation revealed that these defects were linked to the hippocampal dysregulation of neurofibromin-dependent pathways (Provenzano G, et al., 2014a). Specifically, the impaired spatial learning detected in the MWM was associated with reduced neurofibromin expression and increased ERK phosphorylation (pERK) levels in the hilus of *En2*^{-/-} adult mice (Provenzano G, et al., 2014a). Meanwhile, the reduced phosphorylation of synapsin I in the hippocampus was also detected in *En2*^{-/-} mice, before and after MWM (Provenzano G, et al., 2015b).

Moreover, *En2*^{-/-} adult mice also displayed growth hormone (GH) dysfunctions throughout the neuroendocrine axis and the hippocampus. GH is responsible for the synthesis of Insulin-like growth factor 1 (IGF-1), which was found to be associated with ASD (Provenzano G, et al., 2014b). *En2*^{-/-} adult mice exhibited a dysregulation of FMRP-mGluR5 signaling pathway, accompanied by a reduced GABRB3 expression, and this dysregulation may be associated to the “autistic-like” features (Provenzano G, et al., 2015a) .

1.4 Mammalian Visual System

The visual system is the part of the central nervous system by which the animals are able to process and perceive visual details received from the

surroundings. The visual system can detect and interpret visible light information received from the eye to reconstruct a representation of the surrounding environment. It is responsible for a series of complex tasks, which include the process of light reception and the formation of monocular representations; the process of binocular perception buildup from a pair of two dimensional projections; the process of visual objects identification and categorization; the process of assessing distances to and between objects; and the process of guiding body movements responding to the objects seen.

In mammals, the visual system includes the eyes, the optic nerve, the lateral geniculate nucleus (LGN) of the thalamus and the visual cortex. Many mammals, including humans, rely on vision as their primary sense to evaluate their surroundings and guide their behavior. Visual perception starts when light through the cornea and the lens from the surroundings is focused onto the retina, which converts it into neuronal signals. These signals are then mainly sent through the optic nerve to the primary visual cortex via the LGN for further processing.

1.4.1 Retinal development in mammals

The correct development and assembly of seven principal different cell types into the functional architecture of the neural retina is the first step for visual perception of our surroundings. Vertebrate retina starts to develop from optic

vesicles, which derive from the anterior neural plate and proceed to develop into the optic cup. Cell differentiation in the vertebrate retina initiates in the inner layer of the central optic cup and progresses concentrically in a wave-like manner until getting to the peripheral edges of the retina (*Prada C, et al., 1991*). Retinogenesis in the vertebrate retina proceeds in a relatively fixed chronological sequence in which the different types of retinal neurons are generated (Fig. 1.4.1) (*Young R W, et al, 1985*). All retinal types derive from a common population of multipotent retinal progenitor cells (RPCs) residing in the inner layer of the optic cup. During retinogenesis, ganglion cells and horizontal cells differentiate first, followed by cone photoreceptors in overlapping phases, amacrine cells, rod photoreceptors, bipolar cells and, finally, Müller glial cells. Differentiated six main classes of retinal neurons can be further divided into several subclasses. These six types of retinal neurons finally become incorporated into the local neural circuitry which is responsible for the initial step in the visual processing of visual information (*Marquardt T, Gruss P, 2002*).

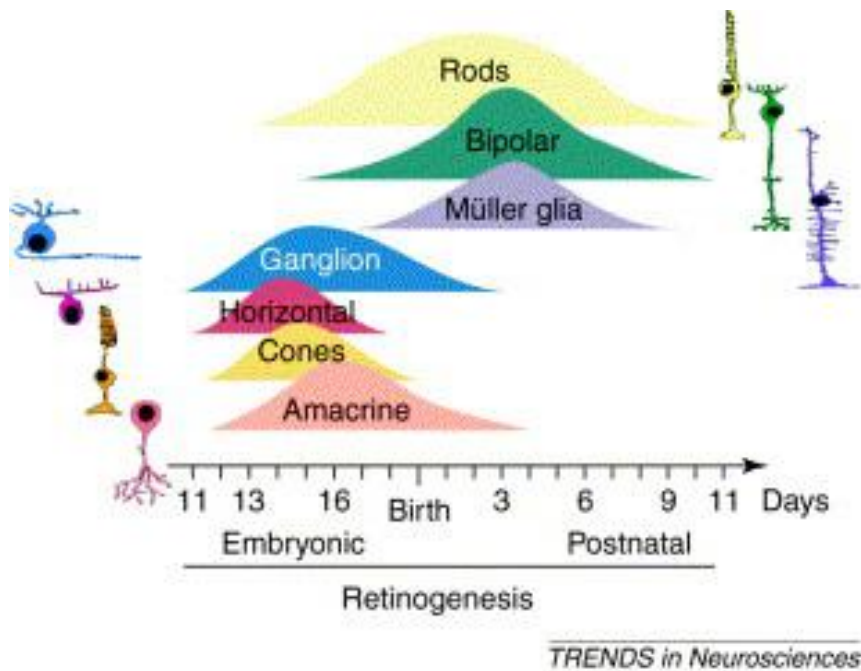


Fig. 1.4.1 Retinal neurogenesis in the vertebrate retina proceeds in a fixed histogenetic sequence. (Marquardt T, Gruss P., 2002).

The process of guiding RPCs towards different cell fates is associated with several extrinsic factors. The first factor is Sonic Hedgehog (Shh) secreted by initially differentiated retinal ganglion cells. Secreted Shh is required to promote the progression of the proximo-distal wave of ganglion cell differentiation and to induce its own expression. During this process, Shh factors have an impact on negatively regulating the ganglion cell genesis following the proximo-distal differentiation wave (Neumann C J, et al., 2000) (Zhang X M, et al., 2001). In addition to Shh, other secreted factors including transforming growth factor- α (TGF- α), epidermal growth factor (EGF) and leukemia inhibitory factor can also have an effect on specifically stimulating the production of some types of retinal cell types, while negatively suppressing the

production of others types of retinal neurons (*Lillien L, 1998*). Another factor, ciliary neurotrophic factor (CNTF), can directly redirect immature postmitotic rod photoreceptors towards the Müller glia fate well after cell cycle exit (*Ezzeddine Z D, et al, 1997*). Apart from the regulation by extrinsic signals in retinal cell differentiation, cell-autonomous factors in RPCs also play a role in mediating changes in the intrinsic responsiveness of RPCs to particular extracellular signals (*Cepko C L, et al., 1996*) (*Livesey F J, et al., 2001*).

1.4.2 Retinal structure

The vertebrate retina is an approximately 150-400 µm thick neural tissue lining at the back of the eye, which is a part of the central nervous system (CNS), deriving embryologically from the neural tube. Therefore, retinal neurons share a lot of common properties with other CNS tissues, while they still possess some specialized properties and proteins which are associated with the retina's specific function in converting light information into nerve signals and further analyzing the image or non-image information.

The retina has a well-organized laminar structure which is conserved in all vertebrate species (*Dowling J E, 1987*) (*Rodieck R W, Rodieck R W, 1998*). Generally, the vertebrate retina contains > 60 types of retinal neurons, which can be classified into five major classes: photoreceptors (3-4 types), horizontal cells (2 types), bipolar cells (10-12 types), amacrine cells (29-30 types), and

ganglion cells (10-15 types) (*Masland R H, 2001*) (*Wässle H, 2004*). There are two major types of photoreceptors cells: rods and cones (*Ebrey T, Koutalos Y, 2001*). In vertebrate retina, there are three subtypes of cone photoreceptors which are sensitive to different spectrum: short-wavelength (S or blue-sensitive) cones, middle-wavelength (M or green-sensitive) cones, and long-wavelength (L or red-sensitive) cones (*Thoreson W B, 2008*). There are 9-11 types of cone bipolar cell, which can be categorized into two major physiological subtypes: cone ON bipolar cells that depolarize to light and cone OFF bipolar cells that hyperpolarize to light, and a single type of rod bipolar cell (*Masland R, 2001*) (*Wässle H, 2004*). In vertebrates, there are two types of horizontal cells, one of them possessing an axon with a finely-branched terminal. However, rats and mice have only one type of horizontal cells, though most mammals have two types of horizontal cells (*Thoreson W B, 2008*). Amacrine cells in vertebrate retina can be grouped into 29 different subtypes based on anatomical and neurochemical criteria (*Masland R, 2001*) (*Wässle H, 2004*). Some specific amacrine cells have well-characterized functions, such as All amacrine cells, which are responsible for transferring rod signals from rod bipolar cells to ganglion cells (*Bloomfield S A, Dacheux R F, 2001*), and starburst amacrine cells, which are supposed to be important in directional selectivity (*Taylor W R, Vaney D I, 2003*). There are 10-15 types of ganglion cells in various species. In primate retina, there are two most common types: M (magnocellular) cells and P (parvocellular) cells (*Thoreson W B, 2008*).

In mouse retina, there are two types of photoreceptors: rods and cones, and the percentage of cones (only short and medium wavelength sensitive cones) was estimated to be approximately 2.8% of the total photoreceptor population (Ortín-Martínez A, et al., 2014), indicating the mouse is rod-dominated. This corresponds to the life style of the mouse, which is a nocturnal animal. Mouse retina only has one type of horizontal cell (Peichl L, et al., 1994), which are B-type axon-bearing horizontal cells (Suzuki H, Pinto L H, 1986), accounting for around 3% of the total cells in the inner nuclear layer (INL) (Jeon et al., 1998). Bipolar cells in mouse retina have at least ten types of cone bipolar cells and one rod bipolar cell type (Famiglietti Jr E V, 1981) (Cohen E, Sterling P, 1990a,b) (Euler T, Wässle H, 1995), comprising 40% of the cell bodies in the INL (Jeon et al., 1998). Amacrine cells in mouse retina were classified into two main types: glycinergic amacrine cells and Gamma-aminobutyric acidergic (GABAergic) amacrine cells, and these two main types account for approximately half of the amacrine cell population. Glycinergic amacrine cells mainly are a type of small-field amacrine cells (Pourcho R G, Goebel D J, 1985) (Menger N, et al., 1998), while GABAergic amacrine cells are a type of wide-field amacrine cells. In addition to glycinergic and GABAergic amacrine cells, there are also dopaminergic and cholinergic amacrine cells in the mouse retina (Wulle I, Schnitzer J, 1989) (Jeon et al., 1998), composing of about 41% of total cells in that layer (Jeon et al., 1998). Apart from the amacrine cells in the INL, there are around 4% of cells in ganglion cells layer are displaced

amacrine cell (*Jeon et al., 1998*). The ganglion cells in the mouse retina are located in the ganglion cells layer (GCL), accounting for the majority of cell in this layer (*Jeon et al., 1998*). Like other species, three nuclear layers in mouse are divided by two plexiform layer: OPL and IPL.

1.5 Sensory Processing in Autism

Sensory processing has been given an increasing attention in both autistic diagnosis and research in recent years (*Robertson C E, Simon B C, 2017*). Sensory symptoms were first figured out in the original report for ASD when ASD was first described (*Asperger H, 1944*) (*Kanner L, 1943*). From then on, sensory processing in ASD was further investigated by different research groups (*Wing L, 1969*) (*Hermelin B, O'connor N, 1970*). Sensory symptoms were also described in some literature written by some autistic patients (*Grandin T, 1992*) (*Grandin T, Johnson C, 2009*) (*Grandin T, 1986*) (*Jackson L, 2002*) (*Williams D, 2009*). Meanwhile, some questionnaires conducted by evaluating parents or caregivers demonstrated particular sensory symptoms in ASD, possibly more frequent than in other neurodevelopmental disorders (*Watling R L, et al., 2001*) (*Rogers S J, 2003*). Sensory processing problems in ASD are mainly reflected in hypersensitivity, avoidance of sensory stimuli, diminished responses to sensory stimulation, and/or sensory seeking behavior. In turn, these symptoms could finally affect the multiple sensory systems

including the visual, auditory, gustatory, olfactory and tactile systems (Ben-Sasson A, 2008) (Cascio C J, et al., 2015) (Foss-Feig J H, et al., 2012) (Klintwall L, et al., 2011) (Lane A E, et al., 2014) (Liss M, et al., 2006) (Marco E J, et al., 2012) (O'Connor K, 2012). Studies in autistic children showed they have an enhanced visually evoked potential (VEP) response to high spatial frequencies, while non-autistic children characterize the facial emotions by using generally low spatial frequency information (Vlamings P H J M, et al., 2010). This observed difference in autistic children is in accordance with previous studies which revealed autistic perception is more detail-oriented, suggesting primary visual processing could also contribute to social and communication deficits in autism (Dakin S, Frith U, 2005) (Happé F, Frith U, 2006) (Mottron L, et al., 2006) (Behrmann M, et al., 2006). Meanwhile, sensory processing abnormalities were also observed in autism mouse models. Studies in *Cntnap2*^{-/-} autistic mice exhibited an abnormal response to sensory stimuli and lack the preference for novel odors which were detected by olfaction-based behavioral test (Gordon A, et al., 2016).

2. AIM OF THE THESIS

Mice lacking the homeobox-containing transcription factor *Engrailed 2* (*En2*^{-/-}) have been proposed as a good animal model for autism spectrum disorders, since they display a series of anatomical and behavioral deficits relevant to autism spectrum disorders, including reduced Purkinje neurons, altered anatomy of the amygdala and a significant loss of forebrain GABAergic interneurons, as well as decreased sociability, enhanced seizure susceptibility and impaired spatial learning and memory (*Joyner A L, et al., 1996*) (*Gharani N, et al., 2004*) (*Benayed R, et al., 2005*) (*Kuemerle B, et al., 2007*) (*Sgadò P, et al., 2013*) (*Tripathi P P, et al., 2009*) (*Provenzano G, et al., 2014*).

A recent study published by our laboratory revealed that *En2*^{-/-} mice displayed an altered disposition of GABAergic circuits in the visual cortex, that might contribute to alter binocularity and plasticity of the visual system, while leaving other visual functional properties (acuity, response latency, receptive field size) unaffected (*Allegra M, et al., 2014*). Besides, preliminary experiments performed in our laboratory suggested that, at cellular level, the retina of *En2*^{-/-} mice showed alterations in the number of specific cell subtypes compared with the retina of WT littermates. More importantly, an increasing number of studies published in the past years indicated that the defects in sensory processing might somehow contribute to the pathogenesis of autism (*Robertson C E, Simon B C, 2017*). Moreover, no available study focused on the investigation

of *En2*^{-/-} mice retina till now. Therefore, we decided to investigate the possible retinal defects in the *En2*^{-/-} mice. We initially examined the expression profile of *En2* gene in the mouse retina. We then characterized the retinal defects of each type of retinal neurons in the *En2*^{-/-} mouse retina. Finally, we evaluated, in collaboration with Prof. Claudia Gargini (University of Pisa), the electrophysiological function of the *En2*^{-/-} mouse retina by electroretinogram (ERG).

In this study, we showed for the first time that *En2* gene is expressed in all nuclear layers of adult mouse retina. We also found that *En2*^{-/-} adult mice showed a significantly decreased number of Calbindin (Calbindin⁺) positive horizontal cells, but a significantly increased number of Calbindin⁺ amacrine/ganglion cells. The number of Brn-3a (Brn-3a⁺) positive ganglion cells displayed no difference in both genotypes. Meanwhile, *En2*^{-/-} adult mice showed a significantly reduced expression of the rod photoreceptor marker rhodopsin at both mRNA and protein levels, and a significant reduction of S-cone photoreceptor S opsin, bipolar cells marker pcp2, GABAergic interneurons marker parvalbumin in mRNA levels. Electroretinogram analysis revealed that the amplitude of the b-wave of the scotopic ERG in *En2*^{-/-} mice showed a significant reduction as compared with controls. Taken together, these data indicated that *En2*^{-/-} mice exhibited retinal defects at molecular and cellular level, and also in the function level.

3. MATERIALS AND METHODS

3.1 Animals

Animals were housed in a 12h light/dark cycle with food and water available *ad libitum*. Mice were anesthetized with chloral hydrate and then sacrificed by cervical dislocation, and all efforts were made to minimize the suffering of animals during the experiments. All experimental procedures were performed in accordance with the European Communities Council Directive 2010/63/EU and were approved by the Italian Ministry of Health and Ethics Committee of the University of Trento. The original *En2* mutants (mixed 129Sv × C57BL/6 genetic background; Joyner et al., 1991) were crossed at least five times into a C57BL/6 background. Heterozygous matings ($En2^{+/-} \times En2^{+/-}$) were used to generate the $En2^{+/+}$ and $En2^{-/-}$ littermates used in this study. The genotypes were determined according to the protocols described on the Jackson Laboratory website (www.jax.org; mouse strain $En2^{tm1Alj}$). Male and female $En2^{+/+}$ and $En2^{-/-}$ age-matched adult (3~5 months), P30 and P10 littermates obtained from heterozygous matings were used in this study.

Table 1 Primers for *En2* mouse line genotyping experiments

Primers	Sequence 5' --> 3'
Common	GCCCACAGACCAAATAGGAG
Wild-type Forward	TGCAAAGGGGACTGTTTAGG
Mutant Forward	ACCGCTTCCTCGTGCTTTAC

3.2 Laser Capture Microdissection (LCM)

Fresh eyes from adult *En2*^{+/+} mice were rapidly enucleated, embedded in OCT (Tissue-Tek®, cat #4583), frozen on dry ice, and stored at -80°C. Frozen tissues were cut into 12 µm thick sections and collected on RNase-free polyethylene naphthalate membrane slides (Leica). The sections were then thawed and immediately fixed in 75% ethanol for 30s, followed by a wash in RNase-free water for 30s, counterstained with hematoxylin and eosin for 45s, followed by two washes in RNase-free water for 30s. Finally, the sections were dehydrated in graded ethanol solutions (75% for 30s, 95% for 30s, and 100% for 30s). After being air-dried for 30min, three retinal layers (ganglion cell layer, inner nuclear layer, and outer nuclear layer) were microdissected on a laser capture microdissection (LCM) system (LMD6500; Leica). Total RNA was extracted from the captured layers by using the PicoPure RNA Isolation Kit (Life Technologies Corp.). On-column digestion with RNase-Free DNase Set (Qiagen) was performed to ensure the removal of possible genomic DNA

contamination. Samples were reversed transcribed and subjected to RT-PCR analysis.

3.3 In Situ Hybridization (ISH)

Adult eyes from *En2^{+/+}* and *En2^{-/-}* mice were rapidly removed, washed in 1xPBS, an incision was made on the cornea with a scalpel, then the eyes were immersion-fixed in 4% PFA for 30min. Subsequently, cornea, lens and sclera were removed from the eyecups in 1xPBS and the retinae were fixed again in 4% PFA for 30min. After fixation, the retinae were washed in 1xPBS, infiltrated with 20% sucrose in 1xPBS overnight at 4°C, then embedded in OCT. 12 µm sections were recovered on commercial Superfrost Plus™ glass slides (Thermo Fisher Scientific, Lot# 030117), dried for 20min, fixed with 4% PFA for 20min, and rinsed three times for 15 min with 1xPBS at room temperature (RT). Sections were rinsed with 0.1 M Triethanolamine (pH 7.5) for 5 min, then treated with a solution of 0.1M Triethanolamine containing 0.25% (v/v) acetic anhydride for 10min at RT, finally washed twice for 10 min with 1xPBS. Hybridization was carried out overnight at 65°C in a humid chamber with digoxigenin-labelled riboprobes (1µg/ml) in hybridization mix (50% formamide, 1 x Denhardt's solution, 10% dextran sulfate, 0.20 M NaCl, 8.9 mM Tris-HCl (pH 7.5), 1.1 mM Tris base, 50 mM EDTA (pH 8.0), 5 mM NaH₂PO₄, 5 mM Na₂HPO₄ and 1 mg/ml yeast tRNA). For the *En2* gene (Genbank ID: NM_010134), *En2* specific DNA fragments of approximately 440bp were

generated by RT-PCR from cDNA reverse transcribed from the total RNA extracted from cerebellar cortex, and antisense riboprobes were generated from the flanking T3 RNA polymerase promoter. The name and sequence of the primers used for *in situ* hybridization are listed in Table 2.

After hybridization, the slides were washed three times in 50% formamide 1x SSC for 45 min at 65°C, then washed twice in 1x MABT (100 mM Maleic Acid, 150 mM NaCl, 0.1% Tween 20, pH7.5) for 1h at RT. Subsequently, the sections were blocked in Blocking Buffer (1x MABT, 20% heat-inactivated goat serum and 2% Roche blocking reagent) for 3h at RT. An anti-digoxigenin-AP conjugated antibody (1:2000; Roche Diagnostics, Lot# 13680323) in Blocking Buffer was incubated overnight at 4°C in a humid chamber. The sections were washed twice in 1x MABT for 1h each time at RT, incubated two times with the alkaline phosphatase staining solution (100 mM NaCl, 50mM MgCl₂, 5 mM Tween 20, 2 mM Tetramisol, 100 mM Tris-HCl, pH9.5) for 20min, then with the alkaline phosphatase staining solution containing NBT/BCIP substrate (1:50, Roche Diagnostics, Lot# 130504421). The reaction was stopped by washes in 1xPBS, graded ethanol, and xylene. The sections were cover-slipped with DPX (SIGMA, Lot# BCBG9434V) and photographed using an AxioCam MRm camera connected to a Zeiss Axio Imager M2 microscope (Carl Zeiss optical company).

3.4 RNA Extraction and Quantitative RT-PCR (RT-qPCR)

Fresh eyes from adult mice were rapidly enucleated after sacrifice, and retinæ were immediately stored in the indicated eppendorf tubes in dry ice. Total RNAs from 3 *En2*^{+/+} and 3 *En2*^{-/-} adult mice eyes were extracted by Nucleospin RNA XS kit (Macherey-Nagel). cDNAs were synthesized from 1µg total RNA by SuperScript VILO cDNA Synthesis Kit (Invitrogen, cat #11754050). Quantitative RT-PCR (RT-qPCR) was performed in a C1000 Thermal Cycler (Bio-Rad) with real-time detection of fluorescence, using the KAPA SYBR FAST Master Mix reagent (KAPA Biosystems). Mouse beta-actin (β -actin) was used as an internal standard for quantification analysis. The name and sequence of all primers used in RT-qPCR are reported in Table 2. Ratios of comparative concentrations of each mRNA with respect to β -actin mRNA were then calculated and plotted as the average of three independent reactions with technical replicates obtained from each RNA sample. Expression analysis was performed using the CFX Manager (BioRad) software. For each marker, RT-qPCR was independently repeated three times using the set of cDNAs samples for statistical analysis.

Table 2 Primers used for RT-qPCR and in situ hybridization experiments.

Gene name	Forward (5'-3')	Reverse (5'-3')
Pcp2	AGGCTTCTTCAACCTGCAGA	CGTTTCTGCATTCCATCCTT
M-opsin	CTCTGCTACCTCCAAGTGTGG	AAGGTATAGGGTCCCCAGCAGA

S-opsin	TGTACATGGTCAACAATCGGA	ACACCATCTCCAGAATGCAAG
Rhodopsin	GCCTGAGGTCAACAACGAAT	GATAACCATGCGGGTGACTT
Parvalbumin	TGCTCATCCAAGTTGCAGG	GCCACTTTTGTCTTTGTCCAG
Beta-actin	AATCGTGCGTGACATCAAAG	AAGGAAGGCTGGAAAAGAGC
En2 ISH	GCGTAATACGACTCACTATAGGGAAAG GGGACTCTTTAGGGTTTC	CGCATTAAACCCTCACTAAAGGGAGAAG ATGATTCCAACCTCGCTCT

3.5.1 Immunohistochemistry on Retinal Sections

For immunolabeling of retinal sections, eyecups were rinsed in 1×PBS, then infiltrated with 20% sucrose overnight, embedded in OCT (Tissue-Tek®, cat #4583), then serially sectioned (12µm thick) using a cryostat (Leica CM1850 UV Cryostat). Sections were blocked in blocking solution (0.5% Triton X-100, 1% BSA and 10% fetal bovine serum (FBS) in 1×PBS) at room temperature for 1 hour followed by overnight incubation at 4°C of primary antibodies in 0.5% Triton X-100, 1% BSA, and 3% FBS in 1×PBS. Primary antibodies used in this study are listed in Table 3. Sections were then washed 3×15min in 1×PBS and incubated 2 hours at room temperature with secondary antibodies, conjugated to either Alexa 488 or Alexa 594. The incubation was then followed by 3×15min washes in 1×PBS and slides mounted using Aqua-Poly/Mount Coverslipping Medium (Polysciences, Inc.).

3.5.2 Whole Mount Immunohistochemistry

For whole mount immunolabeling, eyecups were isolated as described in paragraph (3.3). Subsequently, 4 cuts were performed, reaching 2/3 of the radius, to obtain a 'cross' or 'petal' shape that could remain flat. Whole-mounted retinas were incubated in blocking solution (0.3% Triton X-100 and 5% BSA in 1×PBS) overnight at 4°C followed by 3 days of incubation in 0.1% Triton X-100 and 1% BSA in 1×PBS at 4°C in a stable agitator, with the primary antibody. Primary antibodies used in this study are listed in Table 3. The tissue was then washed 3×15min in 1×PBS and incubated 2 days at 4°C with secondary antibodies, conjugated to either Alexa 488 or Alexa 594. Retinas were then washed 3×15min in 1×PBS and mounted onto glass slides using Aqua-Poly/Mount Mounting Medium (Polysciences, Inc.). For each antibody, whole mount retina IHC was independently performed three or four times using retinas from three different *En2^{+/+}* and *En2^{-/-}* mice.

Table 3 Antibodies used for immunohistochemistry experiments.

Antibodies	Dilution	Cat.
Mouse monoclonal anti-Brn-3a	1:500	MAB1585; Millipore
Rabbit polyclonal anti-Calbinidin D-28k	1:5000	CB38; Swant
Mouse monoclonal anti-Opsin	1:500	O4886; Sigma
Mouse monoclonal anti-PSD 95	1:1000	MABN78; Millipore
Mouse polyclonal Cone Arrestin	1:5000	AB15282; Chemicon
Mouse monoclonal anti-Protein Kinase C	1:100	P5704; Sigma
Donkey anti-mouse Alexa 488	1:1000	Invitrogen
Goat anti-rabbit Alexa 488	1:1000	Invitrogen

Goat anti-rabbit Alexa 594	1:1000	Invitrogen
----------------------------	--------	------------

3.6 Image acquisition and cell counting

Image stacks were acquired using an Axio Observer Z1 microscope (Zeiss) equipped with an AxioCam 503 mono camera. For quantitative analysis of calbindin-positive horizontal cells and amacrine/ganglion cells, and for Brn-3a-positive ganglion cells, full mosaic images of whole mount retinal tissues were acquired by the tile function of the microscope using an EC Plan-Neofluar 20x or 40x objective. Z-plane, exposure time and microscope settings were optimized for each marker. All parameters were then maintained for the acquisition of the full mosaic retina in both genotypes. To count cells, 8 tile images in the central part of each 'petal' of the full retina mosaic were extracted, so that in total 32 tile images/retina have been used to count cells. Cell counting was performed by Columbus software (PerkinElmer) or Image J software (NIH) in a consistent way. Parameters (common threshold, area, split factor, individual threshold, contrast, cell roundness) for defining and selecting the objective cells were optimized for each marker in the Columbus software. All the images from both genotypes for each specific marker were analyzed under the same set of parameters in the Columbus software. Cell counting for calbindin-positive amacrine/ganglion cells was performed manually by using Image J. Cell densities were then plotted as the total counting number of each

specific marker positive cells over total counting area (mm²). For PKC-positive bipolar cells synaptic terminals, the corrected average total cell fluorescence was quantified by Image J software. First, the fluorescent images were converted into an 8-byte image, then the scale bar of the image was defined. The specific region which included all the PKC-positive synaptic terminals of each image was selected by using the rectangular toolbar in image J. Integrated density was automatically quantified by the software. Then the background reading was quantified by selecting the region with background signal. The size of the selected regions for interest signal and background quantification was consistent in all images in both genotypes. The corrected average total cell fluorescence for each image was calculated as follows: the corrected average total cell fluorescence = Integrated Density - (Area of selected cell x Mean fluorescence of background readings). For the outer nuclear layer thickness quantification, we calculate the thickness of cone arrestin positive cone photoreceptors in the whole mount retina by using the z stack function of the fluorescence microscope.

3.7 Protein extraction and Western Blot

Total proteins were extracted from 3 *En2*^{+/+} and 3 *En2*^{-/-} adult mice eyes using a standard protocol under reducing conditions. Samples were homogenized and processed in 1 mL RIPA buffer (50 mM Tris-HCl, pH 7.4; 150 mM NaCl; 1% NP-40; 2 mM EDTA; 2mM PMSF; 5 ug/mL leupeptin; 5 ug/mL pepstatin).

Total protein extracts were separated on NuPAGE™ 4-12% Bis-Tris Protein Gels (Invitrogen, Cat# NP0322BOX), then transferred to 0.2mm Nitrocellulose membranes. The membranes were washed in TBS-T (0.1 M Tris, 0.15 M NaCl, 0.1% Tween 20, pH 7.4) for 10 min and blocked in 5% nonfat dry milk in TBS-T for 1 hour. Then the membranes were incubated overnight at +4 °C with the following antibodies listed in Table 4. After TBS-T wash, the membranes were incubated with the secondary anti-mouse/rabbit HRP antibody for 1h at RT. Immunoblots were revealed by ECL chemiluminescence system (GE Healthcare). The protein expression level was detected using chemiluminescence software (BioRad) and densitometric quantification was performed using Image J (NIH). GAPDH was used as an internal standard for protein quantification analysis.

Table 4 Antibodies used for western blot experiments

Antibodies	Dilution	Cat.
Mouse monoclonal anti-rhodopsin	1:5000	O4886; Sigma
Rabbit polyclonal anti-cone arrestin	1:2000	AB15282; Chemicon
Mouse monoclonal anti-GAPDH	1:5000	sc-32233; Santa Cruz Biotechnology
Donkey anti-rabbit HRP	1:5000	711-035-152; Jackson ImmunoLabs
Donkey anti-Mouse HRP	1:5000	715-035-150; Jackson ImmunoLabs

3.8 Statistical Analysis

All experiments were independently repeated 3/4 times in constant conditions.

Statistical analysis was performed by GraphPad Prism 6 software (GraphPad Software). Student's *t*-test was used (*En2^{+/+}* vs. *En2^{-/-}*), with statistical significance level set at $p < 0.05$.

4. RESULTS

4.1 *En2* expression in adult wild-type mice retina

Previous studies demonstrated that, in the adult mouse brain, *Engrailed 2 (En2)* mRNA is predominantly expressed in the cerebellum and ventral midbrain (Joyner A L, 1996) (Gherbassi D, Simon H H, 2006) and at lower levels also in the hippocampus, somatosensory cortex and visual cortex (Tripathi P P, et al., 2009) (Sgadò P, et al., 2013) (Allegra M, et al., 2014). The retina is a part of the central nervous system, since it derives from the diencephalon, which is subdivided from the forebrain during embryonic development. Therefore, *En2* could also be expressed in the retina. For this reason, we decided to investigate *En2* mRNA expression profile in the mouse retina. In order to describe *En2* expression in retinal tissue, we performed RT-PCR experiments on total RNAs extracted from wild-type adult whole retinas and from the three retinal nuclear layers microdissected by laser capture. Our experiments showed that *En2* mRNA was expressed across the adult retina, in all three isolated nuclear layers (Fig. 4.1A; 4.1B). As expected, *En2* expression was abolished in *En2* KO mice (Fig. 4.1B). These data were also supported by *in situ* hybridization experiments that showed a strong *En2* positive staining in INL and GCL, and a weaker stain in the ONL, of *En2* WT retina and absence of signal in *En2* KO retina (Fig. 4.1C).

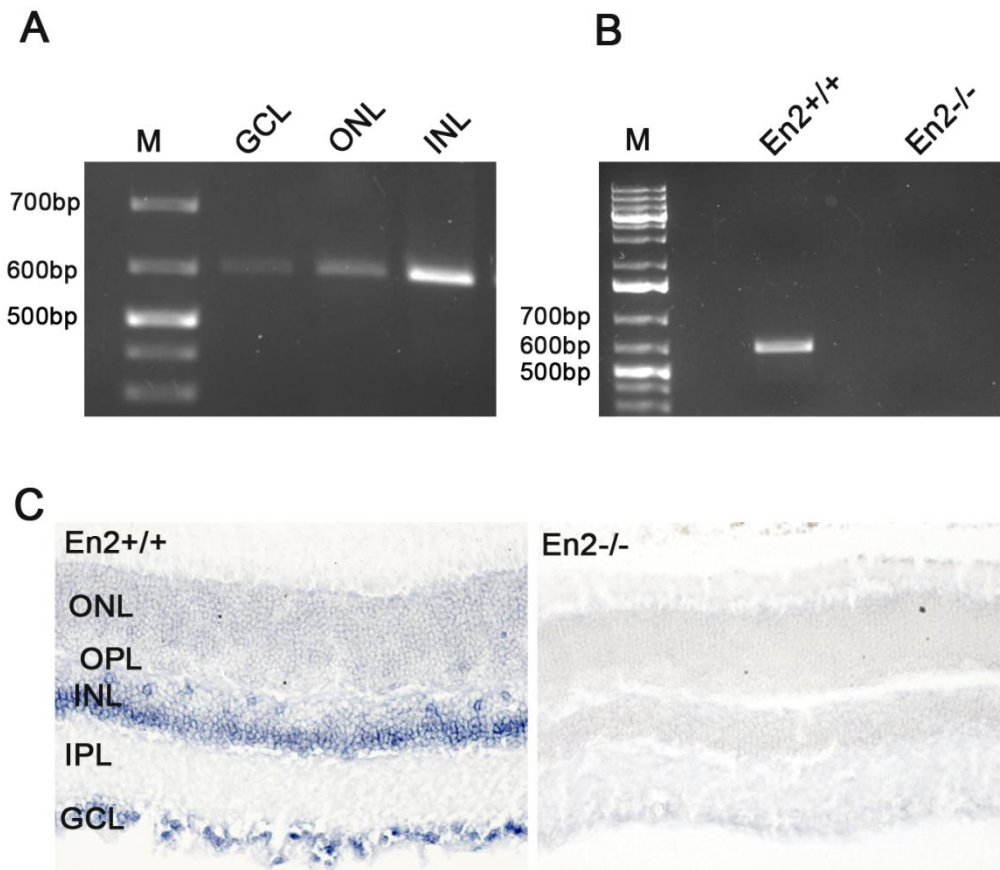


Fig. 4. 1 *En2* mRNA was expressed in the ONL, INL, and GCL of *En2*^{+/+} adult mouse retina, but not in *En2*^{-/-} adult mouse retina. A), RT- PCR generated amplicons of *En2* mRNA in the ganglion cell layer (GCL, lane 2), in the outer nuclear layer (ONL, lane 3), and in the inner nuclear layer (INL, lane 4) collected by laser capture microdissection (LCM). Lane 1 represents the 100 bp Molecular Weight Marker. B), RT-PCR for *En2* mRNA in *En2*^{+/+} (lane 2), and in *En2*^{-/-} adult mice retina (lane 3). C), Representative pictures from *En2 in situ* hybridization on retinal sections showing *En2* positive neurons distributed in all nuclear layers (GCL, INL and ONL) of *En2*^{+/+} adult retinas, but not in those of *En2*^{-/-} adult retinas.

4.2 Reduction of rhodopsin expression in *En2*^{-/-} adult retina

Since we confirmed *En2* expression in the three nuclear layers of the adult mouse retina, we decided to investigate the impact of the knockout of *En2* on retinal anatomy and function and on the different subtypes of retinal neurons. Rod photoreceptors are one of the two photoreceptor types, together with cones, and their cell bodies and nuclei are located in the ONL (Jeon C-J, 1988) (Haverkamp S, 2000). To understand how rod photoreceptors behave in the *En2*^{-/-} mice, we decided to perform immunohistochemistry (IHC) experiments on retinal sections by using a marker specifically labeling rod photoreceptors, rhodopsin. Rhodopsin is a light-sensitive G protein-coupled receptor located on the rod outer segment disk membrane, involved in the phototransduction process (Litman, B. J, Mitchell, D. C, 1996). Rhodopsin antibodies specifically label the outer segment of rod photoreceptors (ROS) in mouse retina (Fig. 4.2A). In the *En2*^{-/-} mice retina, Rhodopsin exhibited a less organized and compacted staining in ONL containing the photoreceptors bodies, but also of the ROS, compared with WT controls (Fig. 4.2A). In order to further understand rhodopsin disorganization in *En2*^{-/-} mice, we performed quantitative RT-PCR (RT- qPCR) experiments on *En2*^{+/+} and *En2*^{-/-} retina. This analysis showed a significant reduction of rhodopsin mRNA content in the eye of *En2*^{-/-} mice compared with age-matched *En2*^{+/+} mice (Fig. 4.2B) ($p < 0.01$, student *t*-test; $n = 3$ replicates experiments of total 3 mice per genotype). To further elucidate whether rhodopsin reduction in mRNA level is also consistent

at the protein level, rhodopsin protein expression in *En2*^{-/-} adult retina was examined by western blot. Rhodopsin western blot unveiled three rhodopsin isoforms in the mouse retina: monomer; dimer and oligomer isoforms (Fig. 4.2C), respectively. In *En2*^{-/-} adult mice, rhodopsin dimer exhibited an obvious reduction compared to *En2*^{+/+} controls (Fig. 4.2C), while the monomer and oligomer isoforms showed no visible difference (Fig. 4.2C). Image J quantification showed that rhodopsin dimer isoform in *En2*^{-/-} adult mouse retina decreased significantly (Fig. 4.2D) ($p < 0.05$, student *t*-test; $n = 3$ *En2*^{+/+} and 3 *En2*^{-/-} mice), while monomer (Fig. 4.2E) and oligomer isoform (Fig. 4.2F) expression demonstrated no significant difference between the two genotypes.

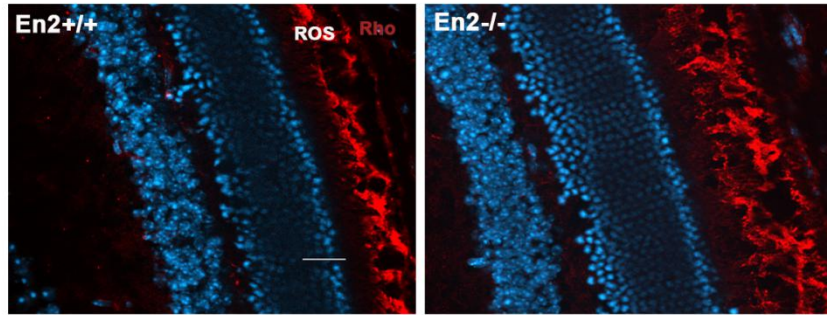
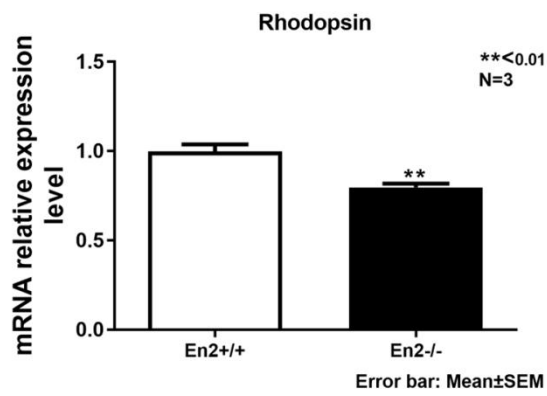
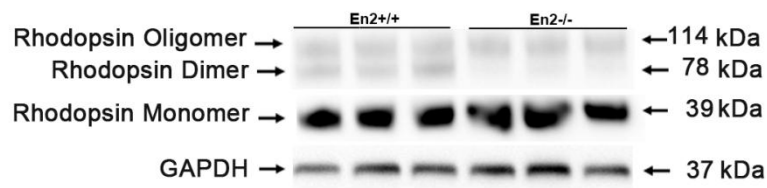
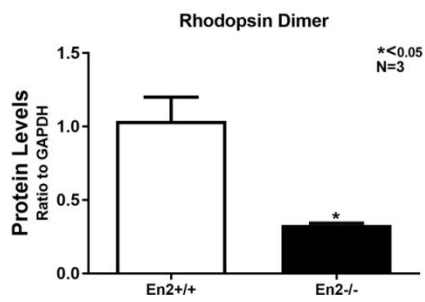
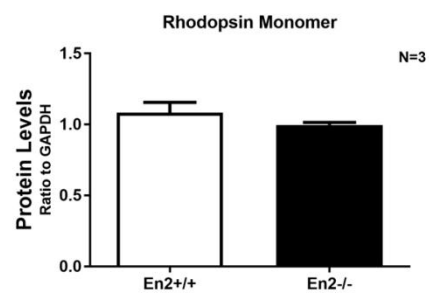
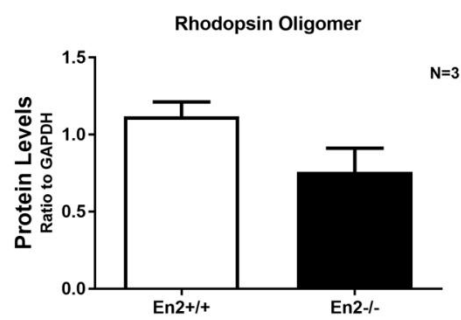
A**B****C****D****E****F**

Fig. 4. 2 Rod photoreceptors in *En2*^{-/-} adult mice. A), Rhodopsin immunohistochemistry in *En2*^{+/+} and *En2*^{-/-} adult retinal sections. B), Relative mRNA expression level of rod photoreceptors specific marker rhodopsin, as obtained by RT-qPCR performed on whole retinas of *En2*^{+/+} and *En2*^{-/-} adult mice. Values were expressed as each marker/ β actin comparative quantitation ratios. C), Representative of rhodopsin immunoblottings from adult mouse retina of both genotypes. Three samples per genotype are shown. GAPDH was used as internal standard. D), Quantification and statistical analysis of rhodopsin dimer (n=3 mice per genotype); E), Quantification and statistical analysis of rhodopsin monomer (n=3 mice per genotype); F), Quantification and statistical analysis of rhodopsin oligomer (n=3 mice per genotype); values in D), E) F) were normalized to GAPDH (Mean \pm S.E.M of 3 replicates from 3 mice per genotype; *p<0.05, Student's *t*-test, *En2*^{+/+} vs. *En2*^{-/-}).

4.3 Decreased expression of S-opsin mRNA in *En2*^{-/-} adult retina

We then investigated the cone photoreceptors component in *En2*^{+/+} and *En2*^{-/-} retina. We performed immunohistochemistry on adult retinal sections with an antibody against cone arrestin (*Chen M, et al., 2013*), a general marker for cone photoreceptors. Cone arrestin antibodies label the outer segment, the inner segment and the synaptic endings of the cone photoreceptors in the mouse retina (Fig. 4.3A). In *En2*^{-/-} adult mice, cone arrestin positive outer segment displayed a subtle disorganization, as compared with *En2*^{+/+} adult controls (Fig. 4.3A), indicating that the loss of *En2* gene in the adult mouse retina may somehow directly or indirectly affect the morphology of cone

photoreceptors. To understand whether the number or organization of photoreceptors cell bodies located in the outer nuclear layer in *En2*^{-/-} mice retina was altered, we decided to measure the ONL thickness by performing whole mount retina IHC using cone arrestin as a reference staining marker. Thickness quantification of the outer nuclear layer revealed that there was no difference between *En2*^{+/+} and *En2*^{-/-} mice (Fig. 4.3E), indicating a normal layering of the outer nuclear layer in *En2*^{-/-} mice.

Mouse cone photoreceptors have two different subtypes: short-wavelength sensitive cones (S-cone) and medium-wavelength sensitive cone (M-cone). In order to characterize the different subtypes of cone photoreceptors in *En2*^{-/-} adult mouse retina more in detail, we performed RT-qPCR analysis with two specific markers: S-and M-opsin. The analysis showed that S-opsin expression in *En2*^{-/-} adult mice displayed a significant decrease as compared to *En2*^{+/+} controls, while M-opsin expression did not vary significantly between the two genotypes (Fig. 4.3B) ($p < 0.05$, student *t*-test; $n = 3$ replicates experiments of total 3 mice per genotype). However, western blots showed that protein expression levels are not consistent with mRNA expression: neither S-opsin nor M-opsin expression showed any statistically significant difference between the two genotypes (Fig. 4.3C; 4.3D).

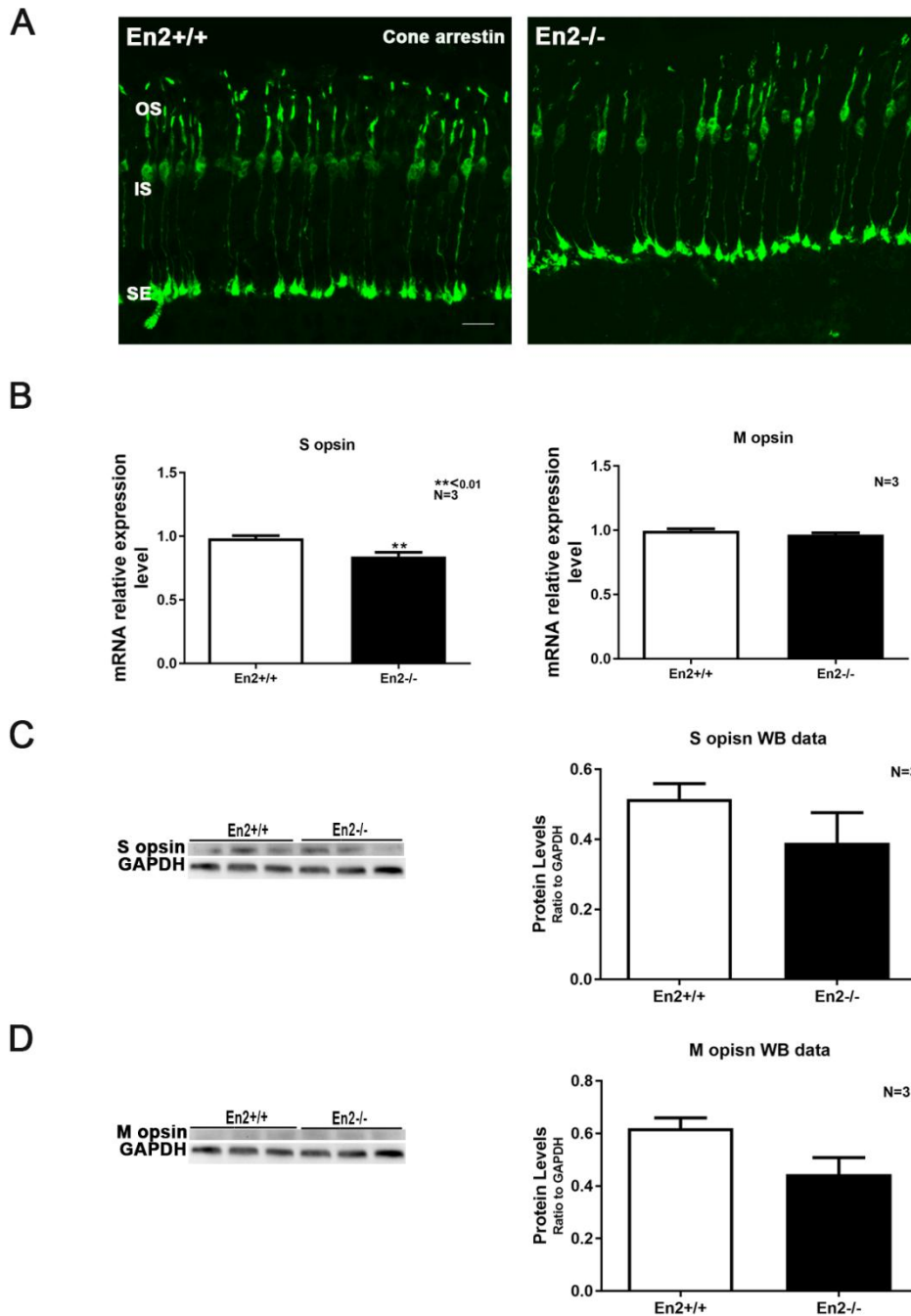


Fig. 4.3 Cone photoreceptors in *En2*^{-/-} adult mice. A), Representative pictures showing cone arrestin-positive photoreceptors in the retina of *En2*^{+/+} and *En2*^{-/-} adult mice. B), Relative mRNA expression level of cone photoreceptors markers S-opsin and M-opsin, as obtained by RT-qPCR performed on the whole retinas of *En2*^{+/+} and *En2*^{-/-} adult mice. Values were expressed as each marker/ β actin comparative quantitation ratios (Mean \pm S.E.M of 3 replicates experiments from total 3 mice per genotype; ** $p < 0.01$, Student's *t*-test, *En2*^{+/+} vs. *En2*^{-/-}). C), Left, representative of S-opsin immunoblottings from adult

mouse retina of both genotypes. Three samples per genotype were shown. GAPDH was used as internal standard. Right, quantification and statistical analysis of S-opsin immunoblotting experiments (n=3 mice per genotype); S-opsin levels were normalized to GAPDH. D), Left, representative M-opsin immunoblottings from adult mice retina of both genotypes. D), Quantification and statistical analysis of the outer nuclear layer in *En2^{+/+}* and *En2^{-/-}* mice. Three samples per genotype were shown. GAPDH was used as internal standard. Right, quantification and statistical analysis of M-opsin immunoblottings experiments (n=3 mice per genotype); M-opsin levels were normalized to GAPDH. E), Quantification and statistical analysis of cone arrestin positive ONL. Scale bar: 50 μ m.

4.4 Reduced *pcp2* expression in bipolar cells in *En2^{-/-}* adult mice

During phototransduction, photoreceptor cells transmit the converted light signals to bipolar cells, located in the inner nuclear layer (INL). To characterize bipolar cells in *En2^{-/-}* mouse retina, we performed RT-qPCR using the bipolar cells specific marker *pcp2*. *Pcp2* is a member of the GoLoco domain-containing family functioning as a cell-type specific modulator for G protein-mediated cell signaling, which is present exclusively in cerebellar Purkinje cells and retinal bipolar cells in the mouse (Xu Y, et al., 2008). The results revealed *pcp2* mRNA expression was significantly reduced, as compared with age-matched *En2^{+/+}* controls (p<0.01, student *t*-test; n=3 replicates experiments of total 3 mice per genotype) (Fig. 4.4 A), indicating that bipolar cells may be disrupted following deletion of the *En2* gene. In order to further investigate whether this molecular deficit could also affect the

morphology of bipolar cells in *En2*^{-/-} mouse retina, we performed IHC on retinal sections with the bipolar cells marker PKC α . PKC α is a type of serine/threonine kinase belonging to a class of classical PKCs, which is implicated in many biological processes, such as proliferation and inflammation (Nakashima S, 2002). PKC α specifically labels rod bipolar cells in the mouse retina (Haverkamp S, et al., 2003). Our PKC α IHC in mouse retinal sections revealed that PKC α specifically labels bipolar cells bodies and synaptic terminals (Fig. 4.4B). In the *En2*^{-/-} adult mouse retina, PKC α positive cells seemed reduced in number and/or in staining intensity as compared to wt controls (Fig. 4.4B). In particular, the synaptic terminals in the *En2*^{-/-} adult mouse retina seemed less dense (Fig. 4.4B). As it was not possible to count positive cells, in order to quantify the possible difference between genotypes, we measured fluorescence density of PKC α positive synaptic terminals. This analysis showed no significant difference in pixel intensity in the synaptic terminals of *En2*^{+/+} and *En2*^{-/-} bipolar cells (Fig. 4.4C). In order to understand whether the synaptic connections between photoreceptors and bipolar cells were disrupted in *En2*^{-/-} adult mice, we chose to perform IHC on retina sections using PSD-95, which labels the synaptic terminals of photoreceptors, at bipolar cell ribbon synapses (dyads) (Koulen P, et al, 1998). PSD-95 is a membrane-associated guanylate kinase (MAGUK) that functions as a scaffolding protein in the excitatory postsynaptic density (PSD) and is a potent regulator of synaptic strength (Chen X, et al., 2011). PSD95 labels the outline

of numerous rod spherules and of five cone pedicles (Haverkamp S, et al., 2003) (Koulen P, et al, 1998). PSD-95 IHC in retinal sections demonstrated that the PSD immunoreactive synaptic terminals showed no difference in both $En2^{+/+}$ and $En2^{-/-}$ (Fig. 4.4D).

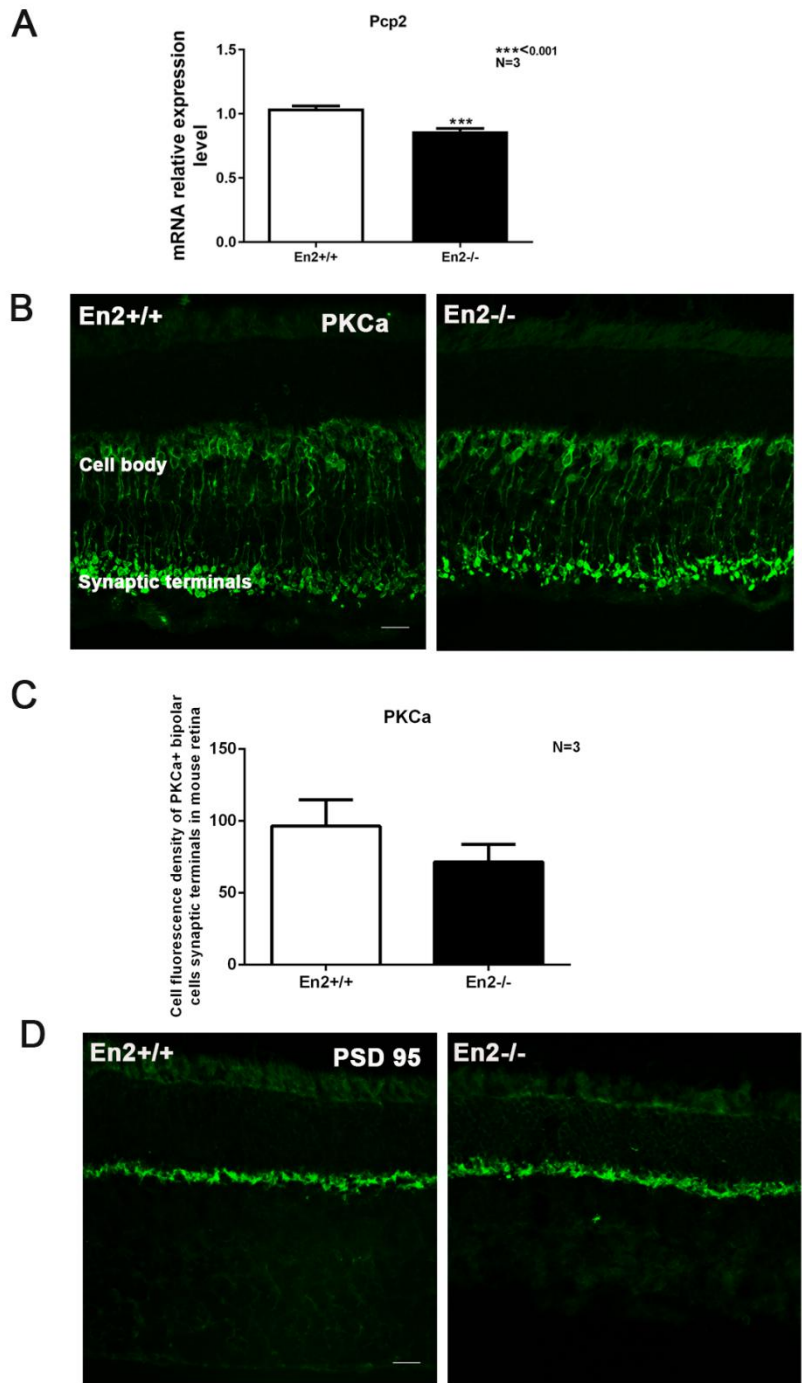


Fig. 4.4 Bipolar cells in *En2*^{-/-} adult mice. A) Relative mRNA expression level of *pcp2*, marker for bipolar cells, as obtained by RT-qPCR performed on the retina of adult *En2*^{+/+} and *En2*^{-/-} mice. Values were expressed as *pcp2*/ β *actin* comparative quantitation ratios (Mean \pm S.E.M of 3 replicates experiments from total 3 mice per genotype; *** $p < 0.001$, Student's *t*-test, *En2*^{+/+} vs. *En2*^{-/-}). B), PKC α immunohistochemistry in *En2*^{-/-} adult retinal sections. C), statistical analysis of cell fluorescence of PKC α positive bipolar cells synaptic terminals in the retinal sections. D), PSD 95 immunohistochemistry in *En2*^{-/-} adult retinal sections. Scale bar: 50 μ m.

4.5 Decreased Calbindin⁺ horizontal cells density in *En2*^{-/-} adult retina

Horizontal cells (HCs) are a type of retinal interneurons that modulate signal transmission between the photoreceptors and bipolar cells (Poché R A, et al., 2007). To better understand if the horizontal cells in the *En2*^{-/-} adult mouse were altered, we performed whole mount retina IHC with a reliable marker for horizontal cells, calbindin. Calbindin is a calcium-binding protein belonging to the family of EF-hand proteins (Wässle H, et al., 1998), which is considered as a marker for horizontal cells, as well as some types of amacrine cells and ganglion cells (Poché R A, et al., 2007). Calbindin whole mount retina IHC showed that calbindin positive (calbindin⁺) horizontal cells density in *En2*^{-/-} adult mouse retina is reduced, as compared to the staining in the *En2*^{+/+} adult mouse retina (Fig. 4.5E). The total number of retinal cells did not change between *En2*^{+/+} and *En2*^{-/-} mice. We thus counted calbindin positive horizontal cells in retinae of mice from both genotypes. Quantification and statistical

analysis of calbindin⁺ horizontal neurons in the inner nuclear layer of retinal whole-mount preparations revealed that the density of calbindin⁺ horizontal cells in *En2*^{-/-} adult mice retina was lower than that in *En2*^{+/+} adult mice retina and this difference was statistically significant (Fig. 4.5F) ($p < 0.05$, student *t*-test, $n = 4$ mice per genotype). To understand when the observed deficits originated, we performed whole mount IHC for calbindin on postnatal day 10 (P10) and postnatal day 30 (P30) retinas. We chose P10, as it is a time point when retinogenesis in the mouse is complete (Yoshida S, *et al.*, 2004), and P30, as the peak of the critical period, an early temporary window of enhanced plasticity (Chen G, *et al.*, 2015). Calbindin whole mount retina IHC on P10 mouse retinae revealed that the density of calbindin⁺ horizontal cells did not differ significantly between genotypes (Fig. 4.5 A, B) ($p > 0.05$, student *t*-test, $n = 3$ mice per genotype). Also at P30, there was no significant difference in the density of calbindin⁺ horizontal cells between genotypes (Fig. 4.5C; 4.5D) ($p > 0.05$, student *t*-test, $n = 3$ mice per genotype).

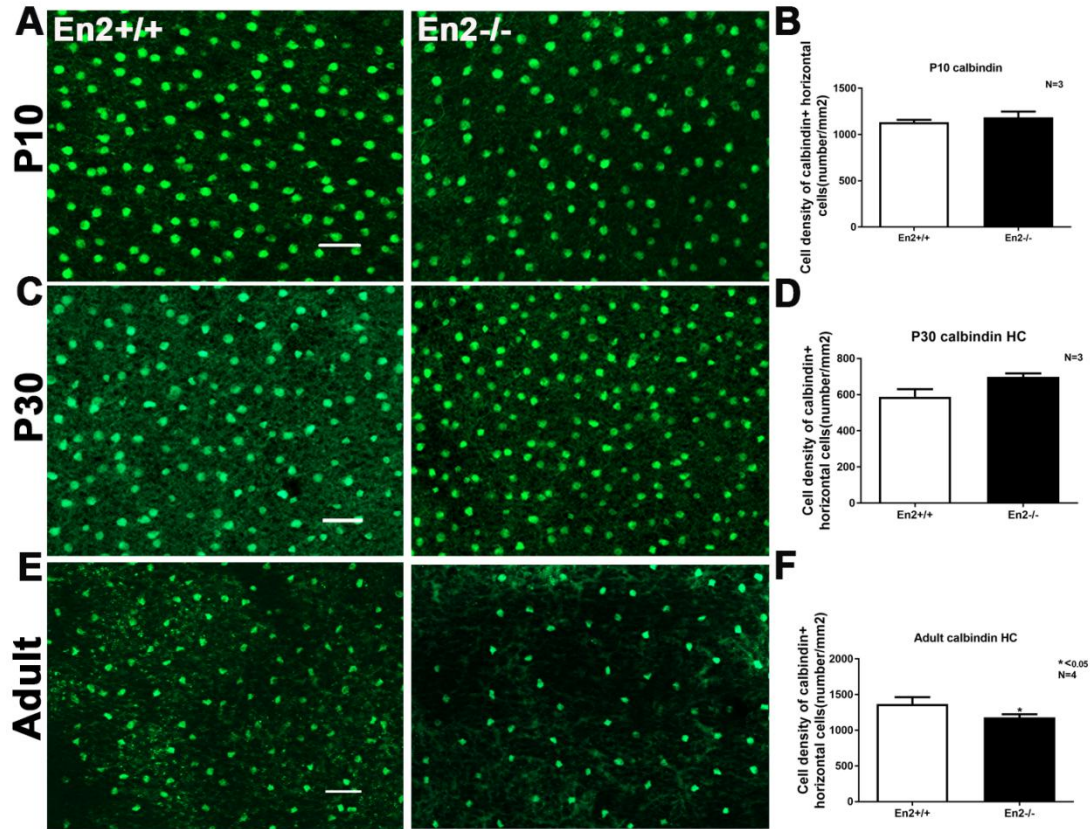


Fig. 4.5 Calbindin⁺ horizontal cells in whole mount retina IHC in *En2^{+/+}* and *En2^{-/-}* adult mice. A), Representative pictures showing Calbindin positive (Calbindin⁺) horizontal cells in the retina of P10 mice from both genotypes. B), Quantitative and statistical analysis of Calbindin⁺ horizontal cells density at P10 mice. C), Representative pictures showing calbindin⁺ horizontal cells in the retina of P30 mice from both genotypes. D), Quantitative and statistical analysis of Calbindin⁺ horizontal cells density at P30 mice. E), Representative pictures showing calbindin⁺ horizontal cells in the retina of adult mice from both genotypes. F), Quantitative and statistical analysis of calbindin⁺ horizontal cells density in adult mice from both genotypes. Values in B), D), F) were expressed as the mean number of positive cells per mm² (Mean ± S.E.M of 3 or 4 replicates experiments from 3 or 4 mice per genotype; *p<0.05, Student's *t*-test, *En2^{+/+}* vs. *En2^{-/-}*). Scale bar: 50 μm.

4.6 Retinal amacrine cells characterization in *En2^{-/-}* mice

In the mouse retina, calbindin immunofluorescence staining recognized not only the horizontal cells in the outer part of the inner nuclear layer (INL), but also labeled some amacrine cells subtypes in the inner part of the inner nuclear layer, and some types of ganglion cells and displaced amacrine cells in the ganglion cells layer (GCL) (Sonntag S, et al., 2012). We selectively acquired all the layers containing calbindin+ amacrine and ganglion cells in the mouse retina and quantified the density of calbindin-labeled amacrine and ganglion cells in *En2*^{-/-} mice retina. Calbindin whole mount retina IHC showed calbindin+ amacrine/ganglion cells in *En2*^{-/-} adult mice were more densely distributed than in the WT controls (Fig. 4.6.1E), and the total number of retinal cells did not change between *En2*^{+/+} and *En2*^{-/-} mice. Quantification and statistical analysis confirmed that in adult mice, the cell density of calbindin+ amacrine/ganglion cells in *En2*^{-/-} mice retina showed a significant increase compared with aged-matched *En2*^{+/+} controls (Fig. 4.6.1F) ($p < 0.05$, student *t*-test, $n = 4$ *En2*^{+/+} and 4 *En2*^{-/-}). At P10, we did not find any difference in the distribution of calbindin positive amacrine/ganglion cells between *En2*^{+/+} and *En2*^{-/-} retina (Fig. 4.6.1 A). Cell counting and statistical analysis further confirmed there was no significant difference in the cell density of calbindin+ amacrine/ganglion cells observed between *En2*^{+/+} and *En2*^{-/-} mice (Fig. 4.6.1B) ($p > 0.05$, student *t*-test, $n = 3$ mice per genotype). Similarly, in P30 mice, calbindin-positive ganglion/amacrine cells were distributed in almost the same way in both genotypes (Fig. 4.6.1C). Cell counting and statistical analysis

validated the absence of any significant difference in the number and distribution of calbindin positive amacrine/ganglion cells between *En2*^{+/+} and *En2*^{-/-} mice (Fig. 4.6.1 D) ($p > 0.05$, student *t*-test, $n = 3$ mice per genotype).

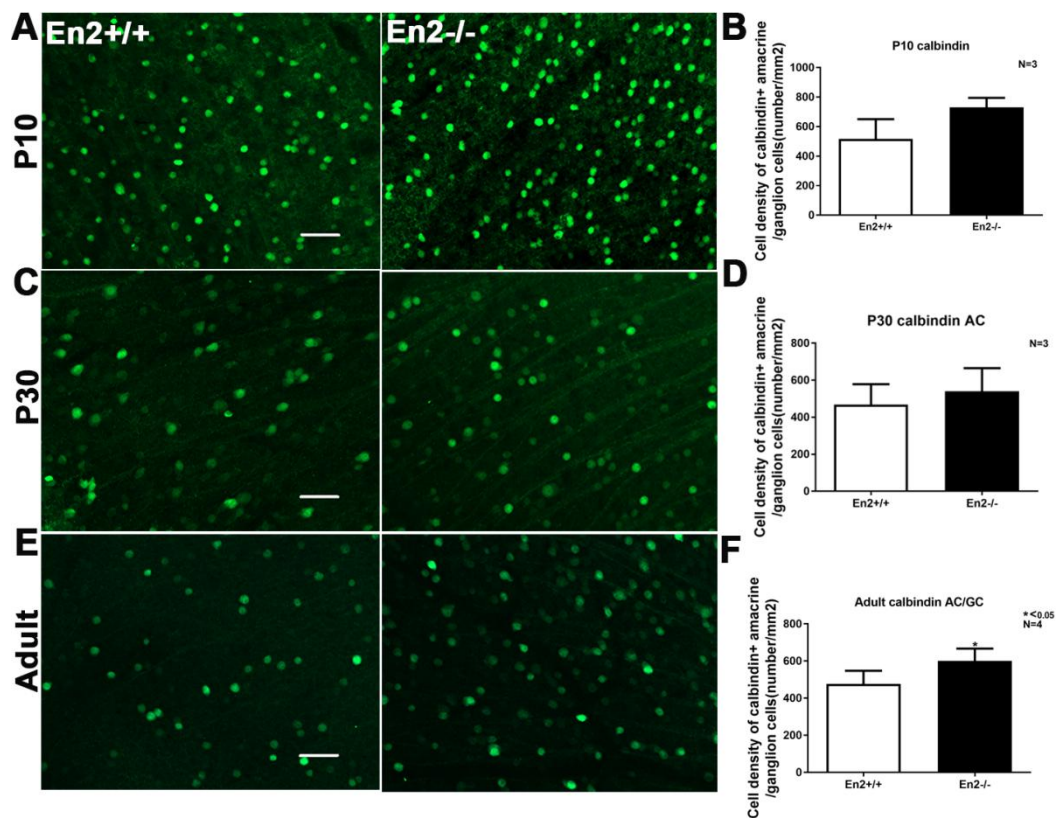


Fig. 4.6.1 Calbindin immunopositive amacrine/ganglion cells in P10, P30 and adult mice. A), Representative pictures showing calbindin positive amacrine/ganglion cells in the retina of P10 mice from both genotypes. B), Quantitative and statistical analysis of calbindin positive amacrine/ganglion cells density in P10 mice. C), Representative pictures showing calbindin positive amacrine/ganglion cells in the retina of P30 mice from both genotypes. D), Quantitative and statistical analysis of calbindin positive amacrine/ganglion cells density in P30 mice. E), Representative pictures showing calbindin positive amacrine/ganglion cells in the retina of adult mice from both genotypes. F), Quantitative and statistical analysis of calbindin positive amacrine/ganglion cells

density in adult mice. Values in B), D), F) were expressed as the mean number of positive cells per mm² (Mean ± S.E.M of 3 or 4 replicates experiments from 3 or 4 mice per genotype; *p<0.05, Student's *t*-test, *En2*^{+/+} vs. *En2*^{-/-}). Scale bar: 50 µm.

As defects in GABAergic interneurons have been reported for different brain areas of *En2*^{-/-} mice (Sgadò P, et al., 2013) (Allegra M, et al., 2014), we questioned whether the increase in calbindin⁺ amacrine/ganglion cells in *En2*^{-/-} adult mouse could originate from defects found specifically in the GABAergic subtypes of amacrine cells. We thus decided to examine GABAergic amacrine cells, by performing RT-qPCR with the GABAergic-specific marker Parvalbumin (PV). PV RT-qPCR results showed a significant increase in PV expression in *En2*^{-/-} mice retina, as compared with age-matched *En2*^{+/+} control mice (Fig. 4.6.2) (p<0.01, student *t*-test, n=3 replicates experiments of 3 mice per genotype), suggesting that GABAergic amacrine cells in the adult mouse retina may also be affected by the *En2* gene deletion.

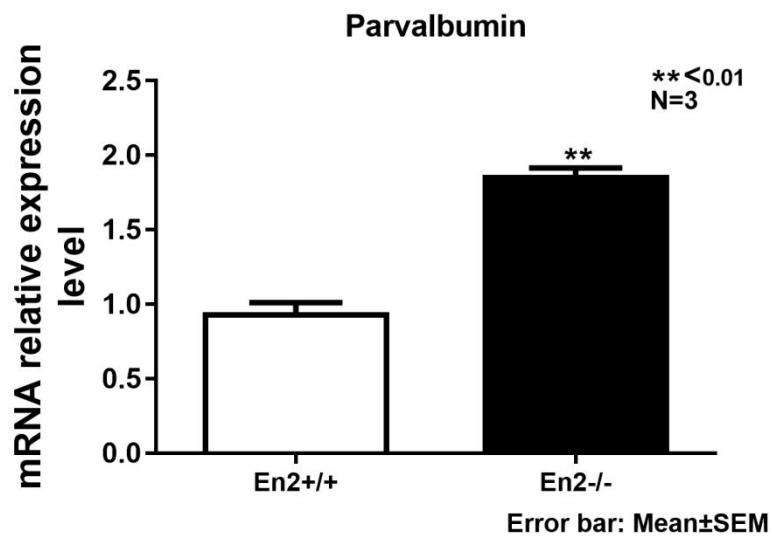


Fig. 4.6.2 Parvalbumin mRNA expression in En2^{+/+} and En2^{-/-} adult mice. Relative mRNA expression level of parvalbumin, marker for GABAergic amacrine cells, as obtained by RT-qPCR performed on the retina of En2^{+/+} and En2^{-/-} adult mice. Values were expressed as PV/ β actin comparative quantitation ratios (Mean \pm S.E.M of 3 replicates experiments from 3 mice per genotype; **p<0.01, Student's *t*-test, En2^{+/+} vs. En2^{-/-}).

4.7 Density of Brn-3a⁺ retinal ganglion cells in En2^{-/-} mice

Since calbindin⁺ amacrine/ganglion cells in En2^{-/-} mice showed a significant increase in density, we wondered if retinal ganglion cells (RGCs) could contribute to this defect. We decided to investigate the RGCs by exploiting the RGCs specific marker Brn-3a, by performing whole mount retina IHC. Brn-3a IHC in adult mouse retina demonstrated there was no evident difference in cell density of Brn-3a⁺ ganglion cells between En2^{+/+} and En2^{-/-} adult mice (Fig. 4.7E), and the total number of retinal cells did not change between En2^{+/+} and

En2^{-/-} mice. Quantification and statistical analysis of the Brn-3a⁺ RGCs cell counts in adult mice confirmed that there was no significant difference in the density of Brn-3a⁺ RGCs (Fig. 4.7F) ($p > 0.05$, student *t*-test, $n = 3$ replicates experiments of 3 mice per genotype). We also performed Brn-3a whole mount retina IHC in P10 and P30 *En2*^{-/-} mice, showing no difference also at these stages (Fig. 4.7A, B, C, D). All above results indicate that the density of Brn-3a⁺ ganglion cells in *En2*^{-/-} mice retina is not affected.

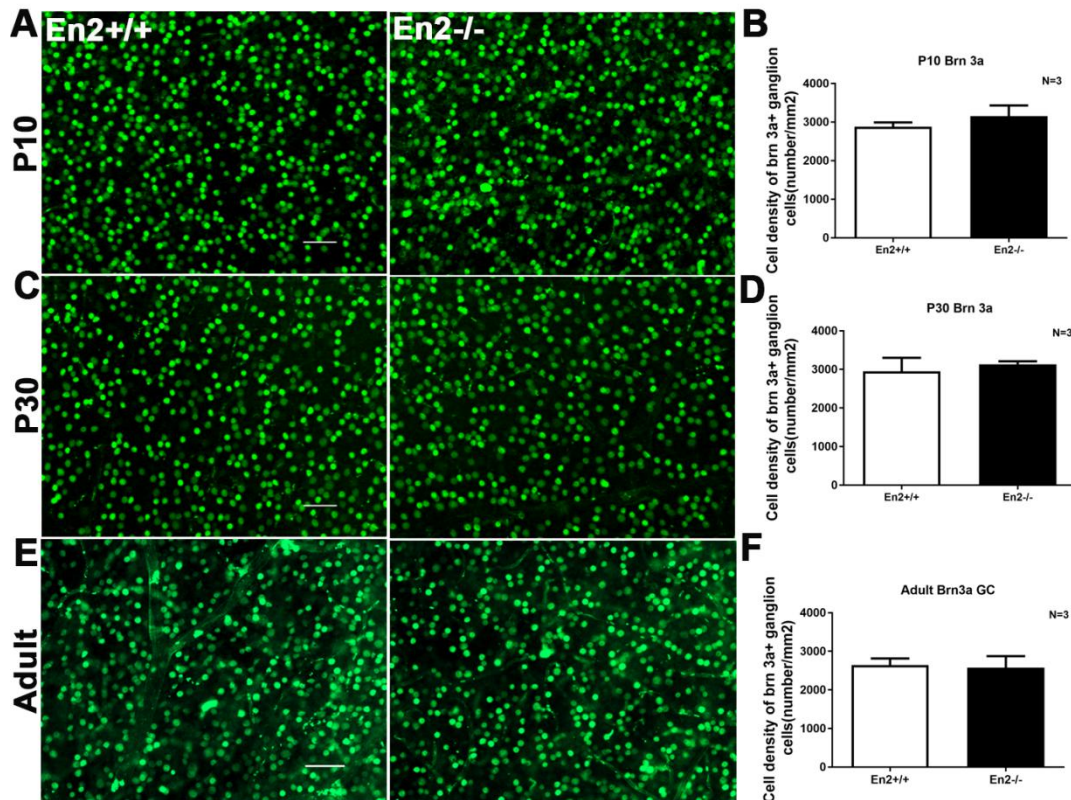


Fig. 4.7 Brn3a immunopositive ganglion cells in P10, P30, and adult *En2*^{-/-} mice. A), Representative pictures showing Brn-3a positive ganglion cells in the retina of P10 mice from both genotypes. B), Quantitative and statistical analysis of Brn-3a positive ganglion cells density in P10 mice. C), Representative pictures showing Brn-3a positive ganglion

cells in the retina of P30 mice from both genotypes. D), Quantitative and statistical analysis of Brn-3a positive ganglion cells density in P30 mice. E), Representative pictures showing Brn3a⁺ ganglion cells in the retina of adult mice from both genotypes. F), Quantitative and statistical analysis of Brn3a⁺ ganglion cells density in adult mice from both genotypes. Values in B), D), F) were expressed as the mean number of positive cells per mm² (Mean ± S.E.M of 3 replicates experiments from 3 mice per genotype; *p<0.05, Student's *t*-test, *En2*^{+/+} vs. *En2*^{-/-}). Scale bar: 50 μm.

4.8 Reduced b-wave in ERGs of *En2*^{-/-} mice under scotopic conditions

The following experiments were carried out by the laboratory of Prof. M.Claudia Gargini (Pharmacology Dep.t, University of Pisa). Although I have not personally carried out the experiments, I participated to the set-up of the experimental design and contributed to data analysis and interpretation. The experiments are shown here so that their significance can be discussed in the following chapter of this thesis.

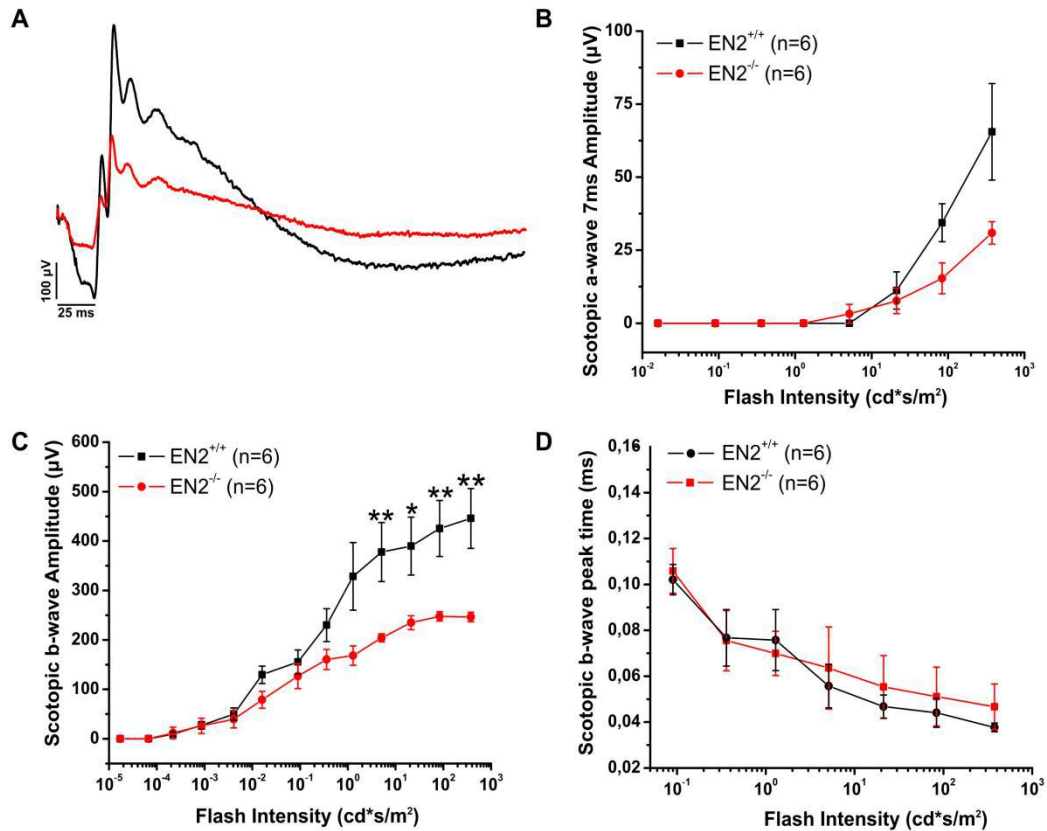


Fig. 4.8.1 Impairment of scotopic retinal function in *En2*^{-/-} mice. A), Representative scotopic flash electroretinogram (ERG) responses from control and *En2*^{-/-} mice. B) and C), Scotopic a-wave and b-wave amplitude as a function of flash intensity from wt and EN2 Ko mice. The traces show that in *En2*^{-/-} mice there is an impairment of ERG function, as the a-wave amplitude is reduced and also the b-wave amplitude is significantly decreased. D), Scotopic b-wave peak time (ms) as a function of flash intensity, the kinetics of the ERG response is the same between WT and *En2*^{-/-} mice. Values expressed as average \pm SEM. Statistical analysis (t-test) * P < 0.05, ** P < 0.01, *** P < 0.001.

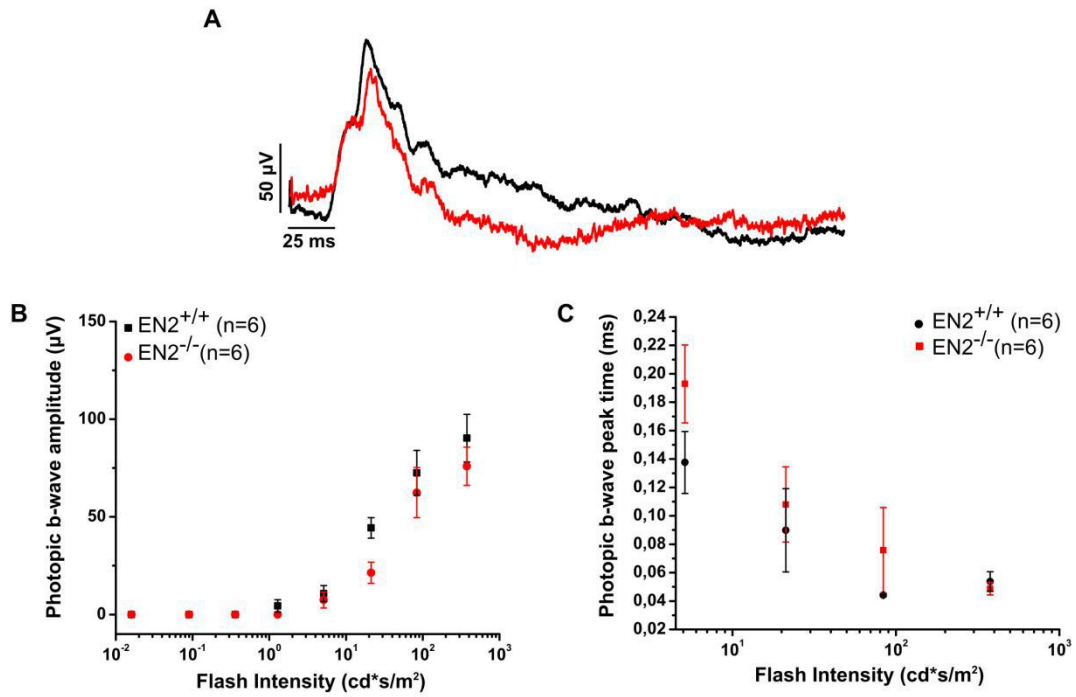


Fig. 4.8.2 Preservation of photopic retinal function in *En2*^{-/-} mice. A), Representative photopic flash electroretinogram (ERG) responses from control and *En2*^{-/-} mice. B), Photopic b-wave amplitude as a function of flash intensity from WT and *En2*^{-/-} mice. The traces show that cones function is preserved in *En2*^{-/-} mice and the ERG amplitude is the same between WT and *En2*^{-/-} mice. C), Photopic b-wave peak time (ms) as a function of flash intensity, the kinetics of ERG response obtained from the cone-pathway is the same between WT and *En2*^{-/-} mice. Values expressed as average \pm SEM.

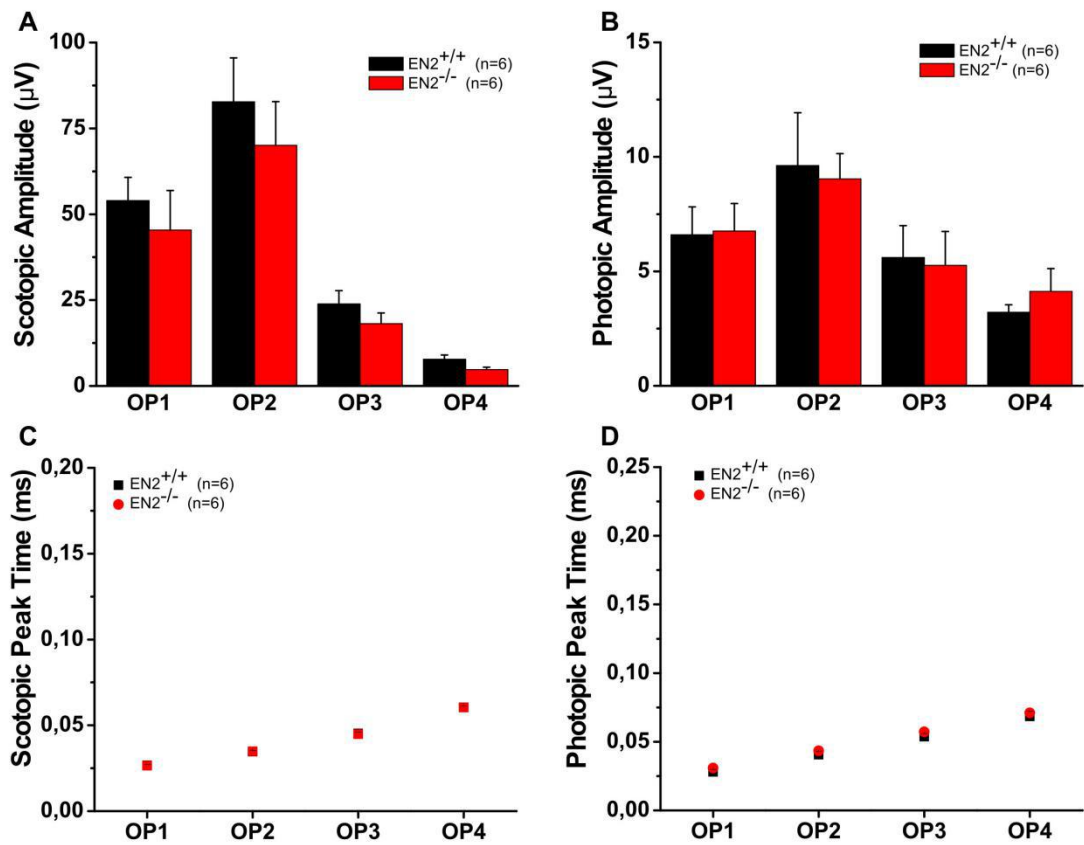


Fig. 4.8.3 Inner retina is not altered in *En2*^{-/-} mice. Average amplitude and implicit time of scotopic (A, C) and photopic (B, D) oscillatory potentials (OP1-OP4) extracted from ERG response to the bright test flash (377cd*s/m²). Both amplitude and kinetic functions show no difference between WT and *En2*^{-/-} mice. Values expressed as average \pm SEM.

5. DISCUSSION

5.1 *En2* expression in adult mouse retina

En2 mRNA is extensively expressed in both the anterior and posterior region of the mouse brain, including the cerebellum, hippocampus and cerebral cortex (Joyner A L, 1996) (Tripathi P P, et al., 2009) (Sgadò P, et al., 2013) (Allegra M, et al., 2014) (Brielmaier J., 2012). Considering *En2* is widely expressed in the brain and the retina is considered as an extension part of the brain, *En2* is possibly expressed in the retina. In this study, we show for the first time that *En2* gene is expressed in the adult wild type mouse retina as we hypothesized (Fig. 4.1B). To be more specific, *En2* is expressed in the three retinal nuclear layers (Fig. 4.1A, 4.1C), as shown independently by RT-PCR and *in situ* hybridization in the retinal tissue, suggesting *En2* plays a role in retinal neurons. Moreover, our results further validated that *En2* gene is expressed in the adult wild type mouse retina, not expressed in the adult *En2*^{-/-} mouse, indicating that the *En2*^{-/-} mice we investigated in this study are real knock-out mice.

5.2 Altered expression of retinal neurons specific markers in the retina of *En2*^{-/-} mice

As *En2* is expressed across all cells layers of the adult mouse retina, we

wondered whether inactivation of *En2* gene could lead to retinal defects. In our study, the reduced mRNA expression of rod photoreceptors specific marker rhodopsin was detected in the *En2*^{-/-} adult mice retina, as compared to age-matched controls (Fig. 4.2B), suggesting that deleting the *En2* gene could directly or indirectly disrupt the expression of rhodopsin. Meanwhile, this disruption was also observed at the protein level of rhodopsin in the *En2*^{-/-} adult mice. To be precise, lacking *En2* specifically affected the expression of rhodopsin dimer in the *En2*^{-/-} mice retina (Fig. 4.2C, 4.2D). This reduction of rhodopsin might be caused by the loss of *En2* transcriptional regulation, as a similar effect was also observed for other homeoprotein transcription factors. In mice lacking homeobox-containing transcription factor *Crx*, a photoreceptor-specific transcription factor that plays a role in the differentiation of photoreceptor cells, photoreceptor outer segment morphogenesis was disrupted, and these cells fail to produce the phototransduction apparatus (*Furukawa T, et al., 1997*). This is due to that *crx* could bind and transactivate the sequence TAATCC/A, which is found upstream of several photoreceptor-specific genes, including the opsin genes from many species, indicating *crx* is essential for the maintenance of mammalian photoreceptors cells (*Freund C L, et al., 1997*). Similar to *Crx*, *En2* homeodomain shows a high-affinity to the sequence TAATTC/A binding site (*Ades S E, Sauer R T, 1994*), and the morphological defects of the outer segment of the rod photoreceptors could also be observed in *En2*^{-/-} mice after loss of *En2* gene.

Specifically, *En2*^{-/-} mice exhibited a less organized and compacted structure of ONL containing the photoreceptors bodies, but also of the ROS, compared with the WT controls (Fig. 4.2A), suggesting that *En2* gene is also likely to be involved in the maintenance of the rod photoreceptors, especially the outer segment. In our study, it is noteworthy that at the protein level, the reduction of the rhodopsin dimer was detected in *En2*^{-/-} adult mice. A recently published study revealed that the rodopsin dimerization is essential for the correct visual pigment rhodopsin folding, maturation, and targeting (Zhang T, et al., 2016), suggesting the dedicated physiological function of rhodopsin could be disrupted in *En2*^{-/-} adult mice due to the failure of dimerization of rhodopsin. Actually, the rod photoreceptors defect is also supported by the electroretinogram (ERG) data in *En2*^{-/-} mice. Scotopic ERG revealed that the amplitude of b-wave in the *En2*^{-/-} mice showed a significant reduction (4.8.1B,C) and a-wave in the *En2*^{-/-} mice is also reduced (Fig 4.8.1B), as compared with the wild type control mice, indicating the functional defects in phototransduction in *En2*^{-/-} mice retina.

Apart from the rod photoreceptor defects, our results also revealed that S cone photoreceptor marker S opsin mRNA displayed a significant reduction in the *En2*^{-/-} mice, while M cone photoreceptors marker M opsin mRNA expression showed no difference in both genotypes (Fig. 4.3B), suggesting that loss of *En2* gene selectively affect the S cone photoreceptors. At protein level, however, the expression level of both S opsin and M opsin showed no

significant difference in *En2*^{+/+} and *En2*^{-/-} mice (Fig. 4.3C, 4.3D). The expression difference in S opsin mRNA and protein level suggests a compensatory mechanism at the translation level of S opsin expression which may have an important implication in the biology of Engrailed 2.

In addition to the photoreceptors, the bipolar cells in *En2*^{-/-} adult mice are also affected. Our results showed that the bipolar cells specific marker *pcp2* mRNA demonstrated a significant reduction as compared with WT age-matched controls (Fig. 4.4 A), suggesting inactivation of *En2* gene in adult mouse retina could have an impact on the *pcp2* expressing bipolar cells. In mouse retina, *pcp2* specifically labeled the rod bipolar cells and some types of ON cone bipolar cells (Xu Y, 2008). To further confirm which subtypes of *pcp2* expressing bipolar cells are disrupted in *En2*^{-/-} adult mice, PKC α immunohistochemistry in *En2*^{-/-} retinal sections was performed. PKC α is a widely used marker for rod bipolar cells in mouse retina (Haverkamp S, Wässle H, 2000). PKC α IHC showed that the number PKC α positive bipolar cells in *En2*^{-/-} mice displayed a visible loss with respect to *En2*^{+/+} mice, though this difference is not statistically significant (Fig. 4.4B, 4.4C). This is probably because the rod bipolar cells are not the only type of bipolar cells contributing to the defects of bipolar cells in *En2*^{-/-} adult mice, and some types of ON cone bipolar cells in *En2*^{-/-} adult mice are also likely to be disrupted. Therefore, to elucidate the defects of *pcp2* expressing bipolar cells, further investigation needs to specifically focus on the ON cone bipolar cells.

5.3 Altered cells density of the horizontal and amacrine cells in *En2*^{-/-} mice retina

Horizontal cells are one of the important players in the mouse retina, that modulate the lateral signal transmission neurotransmission between the photoreceptors and bipolar cells (*Poché R A, et al., 2007*). Particularly, the negative feedback from horizontal cells to cones and direct feed-forward input from horizontal cells to bipolar cells are responsible for many vital processes in the early visual processing in the outer retinae, such as generating center-surround receptive fields that enhance spatial discrimination (*Thoreson W B, Mangel S C, 2012*). Our investigation revealed that the cell density of calbindin positive horizontal cells in *En2*^{-/-} adult mice showed a significant reduction, as compared with the wild type controls (Fig. 4.5E, 4.5F), while there was no significant difference observed in the cell density of calbindin positive horizontal cells in *En2*^{-/-} and *En2*^{+/+} mice at P10 (Fig. 4.5A, 4.5B) and P30 (Fig. 4.5C, Fig. 4.5D) stage, suggesting loss of *En2* might be responsible for the maintenance of the horizontal cells in *En2*^{-/-} mice. A recently published study demonstrated that the horizontal cells in mouse retina play multiple functional roles in retinal circuits (*Chaya T, et al., 2017*). Specifically, loss of the horizontal cells in the adult mice have multiple effects for the mouse retina, including impairing the antagonistic center-surround receptive field formation of RGCs, reducing both the ON and OFF response diversities of RGCs,

impairing the adjustment of the sensitivity to ambient light at the retinal output level, and altering spatial frequency tuning at an individual level (Chaya T, et al., 2017), implying that loss of horizontal cells in *En2*^{-/-} adult mice may eventually affect the spatial vision of the mouse retina. Thus, further studies should be more focused on how the horizontal cells defects could eventually affect vision.

Apart from the defect of the horizontal cells in *En2*^{-/-} adult mice, we also unveiled that the cell density of calbindin positive amacrine/ganglion cells in *En2*^{-/-} adult mice showed a significant increase (Fig. 4.6.1F), as compared with the wild type controls. Meanwhile, we also found that the cells density of Brn 3a positive ganglion cells in *En2*^{-/-} adult mice show no significant alteration, as compared with WT controls (Fig. 4.7E, 4.7F). This means that the observed calbindin positive amacrine/ganglion cells density defects in *En2*^{-/-} adult mice are more likely to originate from the amacrine cells in *En2*^{-/-} adult mice retina. Furthermore, our result also unveiled GABAergic amacrine cells specific marker parvalbumin mRNA expression showed a significant increase, compared with wild type controls (Fig. 4.6.2), implying the loss of *En2* could have a direct or indirect impact on the GABAergic amacrine cells in the mouse retina. Actually, GABAergic interneurons defects have been reported in various regions of the brain when *En2* gene was deleted. Calbindin-expressing Purkinje neurons of the *En2*^{-/-} mice cerebellum showed a decreased cells number (Kuemerle B, et al., 1997) (Orvis G D, et al., 2012) and delayed

maturation (Sudarov A, Joyner A L, 2007). Interestingly, in *En2*^{-/-} mice, the GABAergic interneurons defects are not only limited to the posterior region of the brain, but are also present in more anterior regions of the brain. Targeted inactivation of the *En2* gene in the mouse leads to the decreased PV mRNA and a partial loss of PV interneurons in the hippocampus and in the superficial layers of the somatosensory cortex (Sgadò P, et al., 2013). This was also accompanied by a decreased mRNA expression of specific GABAergic markers in the hippocampus and somatosensory cortex (Sgadò P, et al., 2013), as well as in the visual cortex (Allegra M, et al., 2014). Conversely, in our study, higher mRNA level of GABAergic amacrine cells marker Parvalbumin was detected in the *En2*^{-/-} adult mice retina, suggesting the elevated inhibitory circuit present in the *En2*^{-/-} mice retina. This defect in GABAergic amacrine cells in *En2*^{-/-} mice retina might be explained by the loss of *En2* transcriptional regulation of the expression of the GABAergic gene.

5.4 Impaired scotopic ERG in *En2*^{-/-} adult mice

Scotopic ERG revealed that the a-wave amplitude is reduced and also the b-wave amplitude is significantly decreased in *En2*^{-/-} adult mice, as compared with its wild type controls (Fig. 4.8.1B, C), indicating *En2*^{-/-} adult mice displayed an impaired electrophysiological function. What is the consequence of the electrophysiological defects observed in *En2*^{-/-} mice to the vision still need to be further investigated.

5.5 Retinal defects, visual processing, and autism

Many recent evidences show altered sensory processing in ASD patients and mouse models, whether this can be considered an effect or a cause of other autism-causing neuroanatomical and physiological defects still needs to be understood (Robertson CE, Baron-Cohen S, 2017). In autism mouse models, sensory processing abnormalities have been detected. A previously published study revealed that *Cntnap2*^{-/-} autistic mice exhibited an abnormal response to sensory stimuli and lack preference for novel odors detected by olfaction-based behavioral tests (Gordon A, et al., 2016). Meanwhile, a study in the *Fmr1* KO mice, a mouse model of mental deficiency (MD) with autistic features for Fragile X Syndrome, revealed that the retinal function was altered. To be more specific, the *Fmr1* KO mice displayed a decrease in rhodopsin content and the rod outer segment destabilization, which led to a lower retinal function in the *Fmr1* KO mice (Rossignol R, et al., 2014). This is highly in agreement with what we observed in the *En2* KO mice. In our study, we revealed that *En2*^{-/-} adult mice displayed a reduced expression of rhodopsin in mRNA (Fig. 4.2B) and protein level (Fig. 4.2C, D). Meanwhile, *En2*^{-/-} mice also exhibited the morphological defects in the rod outer segment (Fig. 4.2A). ERG analysis further confirmed the impaired electrophysiological function in the *En2*^{-/-} mice. In the future, we will focus on investigating whether the observed retinal defects could contribute to altered visual perception. If we connect the

retinal defects in *En2*^{-/-} mice to altered visual perception, we could then start investigating whether they present a functional relationship to the other autistic characteristics shown by *En2*^{-/-} mice and in other autistic mouse model, such as *Frm1* KO mice. This study will help us to understand how visual impairments present in autistic patients can contribute to autistic characteristics and finally will benefit the clinical diagnosis for autism spectrum disorders.

6. CONCLUSION AND FUTURE PERSPECTIVES

In this study, we showed *En2* is expressed across all the nuclear layers and *En2*^{-/-} mice displayed some marked retinal defects: altered expression of some retinal neurons markers, including reduced expression of rod photoreceptors marker rhodopsin, decreased expression of S cone photoreceptor marker opsin, reduced expression of bipolar cells marker pcp2, and increased expression of GABAergic amacrine cells marker Parvalbumin. In addition, horizontal cells displayed a significant reduction of cells density in *En2*^{-/-} mice, while amacrine cells showed a significant increase in the cell density. Together, these results indicate *En2*^{-/-} mice exhibited the retinal defects at the molecular and the cellular level, as well as in the physiological function level. In the future, studies should be aimed at linking the observed retinal defects in *En2*^{-/-} to the visual defects of the mouse. Specifically, we will try to evaluate the visual sensory functions which are likely to be affected in the *En2*^{-/-} mice, such as the spatial vision, and direction and orientation selectivity recordings in visual cortex. To this purpose, we will elaborate some electrophysiological/behavior tests specific for the vision sensory functions evaluation.

REFERENCES

- Abrahams B S, Geschwind D H. Advances in autism genetics: on the threshold of a new neurobiology[J]. *Nature reviews genetics*, 2008, 9(5): 341.
- Asperger H. Die Autistischen Psychopathen im Kindesalter [J]. *Archiv für psychiatrie und nervenkrankheiten*, 1944, 117(1): 76-136.
- Alvarez-Fischer D, Fuchs J, Castagner F, et al. Engrailed protects mouse midbrain dopaminergic neurons against mitochondrial complex I insults[J]. *Nature neuroscience*, 2011, 14(10): 1260.
- Allegra M, Genovesi S, Maggia M, et al. Altered GABAergic markers, increased binocularity and reduced plasticity in the visual cortex of Engrailed-2 knockout mice[J]. *Frontiers in cellular neuroscience*, 2014, 8: 163.
- Abbeduto L, McDuffie A, Thurman A J. The fragile X syndrome-autism comorbidity: what do we really know?[J]. *Frontiers in genetics*, 2014, 5: 355.
- Ades S E, Sauer R T. Differential DNA-binding specificity of the engrailed homeodomain: the role of residue 50[J]. *Biochemistry*, 1994, 33(31): 9187-9194.
- Banerjee S, Bhat M, Riordan M. Genetic aspects of autism spectrum disorders: insights from animal models[J]. *Frontiers in cellular neuroscience*, 2014, 8: 58.
- Behrmann M, Thomas C, Humphreys K. Seeing it differently: visual processing in autism[J]. *Trends in cognitive sciences*, 2006, 10(6): 258-264.
- Baio J, Wiggins L, Christensen D L, et al. Prevalence of Autism Spectrum Disorder Among Children Aged 8 Years—Autism and Developmental Disabilities Monitoring Network, 11 Sites, United States, 2010. *MMWR Surveill. Summ.* 63, 1 – 21 (2014).
- Berg J M, Geschwind D H. Autism genetics: searching for specificity and convergence[J]. *Genome biology*, 2012, 13(7): 247.
- Ben- Sasson A, Cermak S A, Orsmond G I, et al. Sensory clusters of toddlers with autism spectrum disorders: Differences in affective symptoms[J]. *Journal of Child Psychology and Psychiatry*, 2008, 49(8): 817-825.

- Betancur C, Sakurai T, Buxbaum JD. The emerging role of synaptic cell-adhesion pathways in the pathogenesis of autism spectrum disorders. *Trends in neurosciences*. 2009 Jul 1;32(7):402-12.
- Berkel, S., Marshall, C. R., Weiss, B., Howe, J., Roeth, R., Moog, U., Rappold, G. A. (2010). Mutations in the SHANK2 synaptic scaffolding gene in autism spectrum disorder and mental retardation. *Nature Genetics*, 42(6), 489 – 91. doi:10.1038/ng.589
- Benayed, R., Gharani, N., Rossman, I., Mancuso, V., Lazar, G., Kamdar, S., Millonig, J. H. (2005). Support for the homeobox transcription factor gene ENGRAILED 2 as an autism spectrum disorder susceptibility locus. *American Journal of Human Genetics*.
- Benayed R, Choi J, Matteson P G, et al. Autism-associated haplotype affects the regulation of the homeobox gene, ENGRAILED 2[J]. *Biological psychiatry*, 2009, 66(10): 911-917.
- Brielmaier J, Matteson P G, Silverman J L, et al. Autism-relevant social abnormalities and cognitive deficits in engrailed-2 knockout mice[J]. *PLoS one*, 2012, 7(7): e40914.
- Bennetto L, Kuschner E S, Hyman S L. Olfaction and taste processing in autism[J]. *Biological psychiatry*, 2007, 62(9): 1015-1021.
- Brewer W J, Edwards J, Anderson V, et al. Neuropsychological, olfactory, and hygiene deficits in men with negative symptom schizophrenia[J]. *Biological Psychiatry*, 1996, 40(10): 1021-1031.
- Bauman M D, Toscano J E, Babineau B A, et al. Emergence of stereotypies in juvenile monkeys (*Macaca mulatta*) with neonatal amygdala or hippocampus lesions[J]. *Behavioral neuroscience*, 2008, 122(5): 1005.
- Baribeau D A, Anagnostou E. A comparison of neuroimaging findings in childhood onset schizophrenia and autism spectrum disorder: a review of the literature[J]. *Frontiers in psychiatry*, 2013, 4: 175.
- Brunet I, Weini C, Piper M, et al. The transcription factor Engrailed-2 guides retinal axons[J]. *Nature*, 2005, 438(7064): 94.
- Bejjani B A, Shaffer L G. Application of array-based comparative genomic hybridization to clinical diagnostics[J]. *The Journal of Molecular Diagnostics*, 2006, 8(5): 528-533.

- Bloomfield S A, Dacheux R F. Rod vision: pathways and processing in the mammalian retina[J]. *Progress in retinal and eye research*, 2001, 20(3): 351-384.
- Bourgeron, Thomas. "From the genetic architecture to synaptic plasticity in autism spectrum disorder." *Nature Reviews Neuroscience* 16.9 (2015): 551.
- Bonati, Maria Teresa, et al. "Evaluation of autism traits in Angelman syndrome: a resource to unfold autism genes." *Neurogenetics* 8.3 (2007): 169-178.
- Christensen J, Grønberg T K, Sørensen M J, et al. Prenatal valproate exposure and risk of autism spectrum disorders and childhood autism[J]. *Jama*, 2013, 309(16): 1696-1703.
- Cepko C L, Austin C P, Yang X, et al. Cell fate determination in the vertebrate retina[J]. *Proceedings of the National Academy of Sciences*, 1996, 93(2): 589-595.
- Cheng Y, Sudarov A, Szulc K U, et al. The Engrailed homeobox genes determine the different foliation patterns in the vermis and hemispheres of the mammalian cerebellum[J]. *Development*, 2010, 137(3): 519-529.
- Cheh M A, Millonig J H, Roselli L M, et al. En2 knockout mice display neurobehavioral and neurochemical alterations relevant to autism spectrum disorder[J]. *Brain research*, 2006, 1116(1): 166-176.
- Carboni G, Tueting P, Tremolizzo L, et al. Enhanced dizocilpine efficacy in heterozygous reeler mice relates to GABA turnover downregulation[J]. *Neuropharmacology*, 2004, 46(8): 1070-1081.
- Cryan J F, Holmes A. Model organisms: the ascent of mouse: advances in modelling human depression and anxiety[J]. *Nature reviews Drug discovery*, 2005, 4(9): 775.
- Cosgaya J M, Aranda A, Cruces J, et al. Neuronal differentiation of PC12 cells induced by engrailed homeodomain is DNA-binding specific and independent of MAP kinases[J]. *Journal of Cell Science*, 1998, 111(16): 2377-2384.
- Chen M, Hombrebueno J R, Luo C, et al. Age-and light-dependent development of localised retinal atrophy in CCL2^{-/-} CX3CR1GFP/GFP mice[J]. *PloS one*, 2013, 8(4): e61381.

- Cohen E, Sterling P. Demonstration of cell types among cone bipolar neurons of cat retina. *Phil. Trans. R. Soc. Lond. B.* 1990a Dec 29;330(1258):305-21.
- Cohen E, Sterling P. Convergence and divergence of cones onto bipolar cells in the central area of cat retina. *Phil. Trans. R. Soc. Lond. B.* 1990b Dec 29;330(1258):323-8.
- Cascio C J, Gu C, Schauder K B, Key A P, Yoder P. Somatosensory event-related potentials and association with tactile behavioral responsiveness patterns in children with ASD. *Brain topography.* 2015 Nov 1;28(6):895-903.
- Chaya T, Matsumoto A, Sugita Y, Watanabe S, Kuwahara R, Tachibana M, Furukawa T. Versatile functional roles of horizontal cells in the retinal circuit. *Scientific reports.* 2017 Jul 17;7(1):5540.
- Chen G, Rasch MJ, Wang R, Zhang XH. Experience-dependent emergence of beta and gamma band oscillations in the primary visual cortex during the critical period. *Scientific reports.* 2015 Dec 9;5:17847.
- Dakin S, Frith U. Vagaries of visual perception in autism[J]. *Neuron*, 2005, 48(3): 497-507.
- Davis C A, Joyner A L. Expression patterns of the homeo box-containing genes *En-1* and *En-2* and the proto-oncogene *int-1* diverge during mouse development[J]. *Genes & Development*, 1988, 2(12b): 1736-1744.
- Durand, C. M., Betancur, C., Boeckers, T. M., Bockmann, J., Chaste, P., Fauchereau, F., Bourgeron, T. (2007). Mutations in the gene encoding the synaptic scaffolding protein SHANK3 are associated with autism spectrum disorders. *Nature Genetics*, 39(1), 25-7.
- DiCicco-Bloom E, Lord C, Zwaigenbaum L, et al. The developmental neurobiology of autism spectrum disorder[J]. *Journal of Neuroscience*, 2006, 26(26): 6897-6906.
- De Rubeis S, Fernández E, Buzzi A, et al. Molecular and cellular aspects of mental retardation in the Fragile X syndrome: from gene mutation/s to spine dysmorphogenesis[M]//*Synaptic plasticity*. Springer, Vienna, 2012: 517-551.
- Dowling J E. *The retina: an approachable part of the brain*[M]. Harvard University Press, 1987.

- Elsabbagh, M. et al. Global prevalence of autism and other pervasive developmental disorders. *Autism Res.* 5, 160-179 (2012).
- Ezzeddine Z D, Yang X, DeChiara T, et al. Postmitotic cells fated to become rod photoreceptors can be respecified by CNTF treatment of the retina[J]. *Development*, 1997, 124(5): 1055-1067.
- Euler T, Wässle H. Immunocytochemical identification of cone bipolar cells in the rat retina[J]. *Journal of Comparative Neurology*, 1995, 361(3): 461-478.
- Ebrey T, Koutalos Y. Vertebrate photoreceptors[J]. *Progress in retinal and eye research*, 2001, 20(1): 49-94.
- Famiglietti Jr E V. Functional architecture of cone bipolar cells in mammalian retina[J]. *Vision research*, 1981, 21(11): 1559-1563.
- Foss-Feig, Jennifer H., Jessica L. Heacock, and Carissa J. Cascio. "Tactile responsiveness patterns and their association with core features in autism spectrum disorders." *Research in autism spectrum disorders* 6.1 (2012): 337-344.
- Fjose A, Eiken H G, Njølstad P R, et al. A zebrafish engrailed-like homeobox sequence expressed during embryogenesis[J]. *FEBS letters*, 1988, 231(2): 355-360.
- Fernandez T, Morgan T, Davis N, et al. Disruption of contactin 4 (CNTN4) results in developmental delay and other features of 3p deletion syndrome[J]. *The American Journal of Human Genetics*, 2004, 74(6): 1286-1293.
- Freund C L, Gregory-Evans C Y, Furukawa T, et al. Cone-rod dystrophy due to mutations in a novel photoreceptor-specific homeobox gene (CRX) essential for maintenance of the photoreceptor[J]. *Cell*, 1997, 91(4): 543-553.
- Furukawa T, Morrow E M, Cepko C L. Crx, a novel otx-like homeobox gene, shows photoreceptor-specific expression and regulates photoreceptor differentiation[J]. *Cell*, 1997, 91(4): 531-541
- Gordon A, Salomon D, Barak N, et al. Expression of Cntnap2 (Caspr2) in multiple levels of sensory systems[J]. *Molecular and Cellular*

- Neuroscience, 2016, 70: 42-53.
- Grandin T. An inside view of autism[M]//High-functioning individuals with autism. Springer, Boston, MA, 1992: 105-126.
- Grandin T, Johnson C. Animals in translation: Using the mysteries of autism to decode animal behavior[M]. SUNY Press, 2009.
- Grandin T. Emergence, labeled autistic[M]. Academic Therapy Pubns, 1986.
- Geschwind D H, Levitt P. Autism spectrum disorders: developmental disconnection syndromes. Current opinion in neurobiology. 2007 Feb 1;17(1):103-11.
- Gadad BS, Hewitson L, Young KA, German DC. Neuropathology and animal models of autism: genetic and environmental factors. Autism research and treatment. 2013.
- Gherbassi, D. and Simon H. H. The engrailed transcription factors and the mesencephalic dopaminergic neurons. Parkinson' s Disease and Related Disorders. Springer, Vienna, 2006. 47-55.
- Gharani N, Benayed R, Mancuso V, et al. Association of the homeobox transcription factor, ENGRAILED 2, 3, with autism spectrum disorder[J]. Molecular psychiatry, 2004, 9(5): 474.
- Gibert J M. The evolution of engrailed genes after duplication and speciation events[J]. Development genes and evolution, 2002, 212(7): 307-318.
- Gardner C A, Darnell D K, Poole S J, et al. Expression of an engrailed - like gene during development of the early embryonic chick nervous system[J]. Journal of neuroscience research, 1988, 21(2 - 4): 426-437.
- Gilby K L, O'Brien T J. Epilepsy, autism, and neurodevelopment: kindling a shared vulnerability?[J]. Epilepsy & Behavior, 2013, 26(3): 370-374.
- Gogolla N, LeBlanc J J, Quast K B, et al. Common circuit defect of excitatory-inhibitory balance in mouse models of autism[J]. Journal of neurodevelopmental disorders, 2009, 1(2): 172.
- Haverkamp S, Wässle H. Immunocytochemical analysis of the mouse retina[J]. Journal of Comparative Neurology, 2000, 424(1): 1-23.
- Happé F, Frith U. The weak coherence account: detail-focused cognitive style

- in autism spectrum disorders[J]. Journal of autism and developmental disorders, 2006, 36(1): 5-25.
- Hermelin B, O'connor N. Psychological experiments with autistic children[J]. 1970.
- Hatton, D. D., Sideris, J., Skinner, M., Mankowski, J., Bailey, D. B., Roberts, J., Mirrett, P. (2006). Autistic behavior in children with fragile X syndrome: prevalence, stability, and the impact of FMRP. American Journal of Medical Genetics. Part A, 140A(17), 1804 – 13.
- Horsthemke B, Buiting K (2006) Imprinting defects on human chromosome 15. Cytogenet Genome Res 113:292 – 299.
- Herrup, Karl, et al. The genetics of early cerebellar development: networks not pathways. Progress in brain research 148 (2005): 21-27
- Hemmati-Brivanlou A, De la Torre J R, Holt C, et al. Cephalic expression and molecular characterization of Xenopus En-2[J]. Development, 1991, 111(3): 715-724.
- Hrabovska S V, Salyha Y T. Animal Models of Autism Spectrum Disorders and Behavioral Techniques of their Examination[J]. Neurophysiology, 2016, 48(5): 380-388.
- Haznedar M M, Buchsbaum M S, Wei T C, et al. Limbic circuitry in patients with autism spectrum disorders studied with positron emission tomography and magnetic resonance imaging[J]. American Journal of Psychiatry, 2000, 157(12): 1994-2001.
- Hutsler J J, Zhang H. Increased dendritic spine densities on cortical projection neurons in autism spectrum disorders[J]. Brain research, 2010, 1309: 83-94.
- Haverkamp S, Ghosh K K, Hirano A A, et al. Immunocytochemical description of five bipolar cell types of the mouse retina[J]. Journal of Comparative Neurology, 2003, 455(4): 463-476.
- Jeon C J, Strettoi E, Masland R H. The major cell populations of the mouse retina[J]. Journal of Neuroscience, 1998, 18(21): 8936-8946.
- Jackson L. Freaks, geeks and Asperger syndrome: A user guide to adolescence[M]. Jessica Kingsley Publishers, 2002.

- Joyner, A. L., Martin, G. R. (1987). En-1 and En-2, two mouse genes with sequence homology to the *Drosophila* engrailed gene: expression during embryogenesis. *Genes & Development*, 1(1), 29-38.
- Joyner A L. Engrailed, Wnt and Pax genes regulate midbrain-hindbrain development[J]. *Trends in Genetics*, 1996, 12(1): 15-20.
- Jiyeon C, S. K. T. R. P. G. M. and J. H. M. (2011). Autism Spectrum Disorders - From Genes to Environment. (T. Williams, Ed.). InTech.
- Joyner A L, Kornberg T, Coleman K G, et al. Expression during embryogenesis of a mouse gene with sequence homology to the *Drosophila* engrailed gene[J]. *Cell*, 1985, 43(1): 29-37.
- Joyner A L, Herrup K, Auerbach B A, et al. Subtle cerebellar phenotype in mice homozygous for a targeted deletion of the En-2 homeobox[J]. *Science*, 1991, 251(4998): 1239-1243.
- James S J, Shpyleva S, Melnyk S, et al. Elevated 5-hydroxymethylcytosine in the Engrailed-2 (EN-2) promoter is associated with increased gene expression and decreased MeCP2 binding in autism cerebellum[J]. *Translational psychiatry*, 2014, 4(10): e460.
- Joliot A, Maizel A, Rosenberg D, et al. Identification of a signal sequence necessary for the unconventional secretion of Engrailed homeoprotein[J]. *Current Biology*, 1998, 8(15): 856-863.
- Kanner L. Autistic disturbances of affective contact[J]. *Nervous child*, 1943, 2(3): 217-250.
- Klintwall, L., Holm, A., Eriksson, M., Carlsson, L. H., Olsson, M. B., Hedvall, Å., Fernell, E. (2011). Sensory abnormalities in autism: a brief report. *Research in developmental disabilities*, 32(2), 795-800.
- Kuemerle B, Zanjani H, Joyner A, et al. Pattern Deformities and Cell Loss in Engrailed-2 Mutant Mice Suggest Two Separate Patterning Events during Cerebellar Development[J]. *Journal of Neuroscience*, 1997, 17(20): 7881-7889.
- Kuemerle B, Gulden F, Cherosky N, et al. The mouse Engrailed genes: a window into autism[J]. *Behavioural brain research*, 2007, 176(1): 121-132.
- Kemper T L, Bauman M. Neuropathology of infantile autism[J]. *Journal of neuropathology and experimental neurology*, 1998, 57(7): 645.

- Kalueff A V, Gebhardt M, Stewart A M, et al. Towards a comprehensive catalog of zebrafish behavior 1.0 and beyond[J]. *Zebrafish*, 2013, 10(1): 70-86.
- Koulen P, Fletcher E L, Craven S E, et al. Immunocytochemical localization of the postsynaptic density protein PSD-95 in the mammalian retina[J]. *Journal of Neuroscience*, 1998, 18(23): 10136-10149.
- Levitt P, Campbell D B. The genetic and neurobiologic compass points toward common signaling dysfunctions in autism spectrum disorders [J]. *The Journal of clinical investigation*, 2009, 119(4): 747-754.
- Lillien L. Neural progenitors and stem cells: mechanisms of progenitor heterogeneity[J]. *Current opinion in neurobiology*, 1998, 8(1): 37-44.
- Livesey F J, Cepko C L. Vertebrate neural cell-fate determination: lessons from the retina[J]. *Nature Reviews Neuroscience*, 2001, 2(2): 109.
- Lane, Alison E., Cynthia A. Molloy, and Somer L. Bishop. Classification of children with autism spectrum disorder by sensory subtype: A case for sensory-based phenotypes. *Autism Research* 7, no. 3 (2014): 322-333.
- Liss M, Saulnier C, Fein D, Kinsbourne M. Sensory and attention abnormalities in autistic spectrum disorders. *Autism*. 2006 Mar;10(2):155-72.
- Lintas C, Persico AM. Autistic phenotypes and genetic testing: state-of-the-art for the clinical geneticist. *J Med Genet*2009;46:1 – 8.
- Logan C, Hanks M C, Noble - Topham S, et al. Cloning and sequence comparison of the mouse, human, and chicken engrailed genes reveal potential functional domains and regulatory regions[J]. *genesis*, 1992, 13(5): 345-358.
- Liu W S, Pesold C, Rodriguez M A, et al. Down-regulation of dendritic spine and glutamic acid decarboxylase 67 expressions in the reelin haploinsufficient heterozygous reeler mouse[J]. *Proceedings of the National Academy of Sciences*, 2001, 98(6): 3477-3482.
- Levitas-Djerbi T, Appelbaum L. Modeling sleep and neuropsychiatric disorders in zebrafish[J]. *Current opinion in neurobiology*, 2017, 44: 89-93.
- Litman BJ, Mitchell DC. A role for phospholipid polyunsaturation in modulating membrane protein function. *Lipids*. 1996 Mar 1;31(1):S193-7.

- Miles, J. H. et al. Essential versus complex autism: definition of fundamental prognostic subtypes. *Am. J. Med. Genet. A* 135, 2005,171 – 180 .
- Mottron L, Dawson M, Soulieres I, et al. Enhanced perceptual functioning in autism: an update, and eight principles of autistic perception[J]. *Journal of autism and developmental disorders*, 2006, 36(1): 27-43.
- Marco EJ, Khatibi K, Hill SS, Siegel B, Arroyo MS, Dowling AF, Neuhaus JM, Sherr EH, Hinkley LN, Nagarajan SS. Children with autism show reduced somatosensory response: an MEG study. *Autism Research*. 2012 Oct 1;5(5):340-51.
- Miles JH. Autism spectrum disorders—a genetics review. *Genetics in Medicine*. 2011 Apr;13(4):278.
- Moon J, Beaudin A E, Verosky S, et al. Attentional dysfunction, impulsivity, and resistance to change in a mouse model of fragile X syndrome[J]. *Behavioral neuroscience*, 2006, 120(6): 1367.
- Macri S, Biamonte F, Romano E, et al. Perseverative responding and neuroanatomical alterations in adult heterozygous reeler mice are mitigated by neonatal estrogen administration[J]. *Psychoneuroendocrinology*, 2010, 35(9): 1374-1387.
- Mostofsky S H, Powell S K, Simmonds D J, et al. Decreased connectivity and cerebellar activity in autism during motor task performance[J]. *Brain*, 2009, 132(9): 2413-2425.
- Minschew N J, Williams D L. The new neurobiology of autism: cortex, connectivity, and neuronal organization[J]. *Archives of neurology*, 2007, 64(7): 945-950.
- Meshalkina D A, Kizlyk M N, Kysil E V, et al. Zebrafish models of autism spectrum disorder[J]. *Experimental neurology*, 2017.
- McCammon J M, Sive H. Challenges in understanding psychiatric disorders and developing therapeutics: a role for zebrafish[J]. *Disease models & mechanisms*, 2015, 8(7): 647-656.
- Morata G, Lawrence P A. Control of compartment development by the engrailed gene in *Drosophila*[J]. *Nature*, 1975, 255(5510): 614-617.
- Masland R H. Neuronal diversity in the retina[J]. *Current opinion in neurobiology*, 2001, 11(4): 431-436.

- Manzi B, Loizzo A L, Giana G, et al. Autism and metabolic diseases[J]. Journal of Child Neurology, 2008, 23(3): 307-314.
- Marquardt T, Gruss P. Generating neuronal diversity in the retina: one for nearly all. Trends in neurosciences. 2002 Jan 1;25(1):32-8.
- Menger N, Pow DV, Wässle H. Glycinergic amacrine cells of the rat retina. Journal of Comparative Neurology. 1998 Nov 9;401(1):34-46.
- Morgan R. Engrailed: Complexity and economy of a multi - functional transcription factor[J]. FEBS letters, 2006, 580(11): 2531-2533.
- McCarroll SA, Altshuler DM. Copy-number variation and association studies of human disease. Nature genetics. 2007 Jun 27;39:S37.
- Newschaffer C J, Croen L A, Daniels J, et al. The epidemiology of autism spectrum disorders[J]. Annu. Rev. Public Health, 2007, 28: 235-258
- Novarino G, El-Fishawy P, Kayserili H, et al. Mutations in BCKD-kinase lead to a potentially treatable form of autism with epilepsy[J]. Science, 2012: 1224631.
- Neumann C J, Nuesslein-Volhard C. Patterning of the zebrafish retina by a wave of sonic hedgehog activity[J]. Science, 2000, 289(5487): 2137-2139.
- Nédélec S, Foucher I, Brunet I, et al. Emx2 homeodomain transcription factor interacts with eukaryotic translation initiation factor 4E (eIF4E) in the axons of olfactory sensory neurons[J]. Proceedings of the National Academy of Sciences of the United States of America, 2004, 101(29): 10815-10820.
- Nakashima S. Protein kinase C α (PKC α): regulation and biological function[J]. The Journal of Biochemistry, 2002, 132(5): 669-675.
- O'Connor K. Auditory processing in autism spectrum disorder: a review. Neuroscience & Biobehavioral Reviews. 2012 Feb 1;36(2):836-54.
- Orvis G D, Hartzell A L, Smith J B, et al. The engrailed homeobox genes are required in multiple cell lineages to coordinate sequential formation of fissures and growth of the cerebellum[J]. Developmental biology, 2012, 367(1): 25-39.
- Ortín-Martínez A, Nadal-Nicolás F M, Jiménez-López M, et al. Number and

distribution of mouse retinal cone photoreceptors: differences between an albino (Swiss) and a pigmented (C57/BL6) strain[J]. PLoS One, 2014, 9(7): e102392.

Peça J, Feliciano C, Ting J T, et al. Shank3 mutant mice display autistic-like behaviours and striatal dysfunction[J]. Nature, 2011, 472(7344): 437.

Prada C, Puga J, Pérez - Méndez L, et al. Spatial and temporal patterns of neurogenesis in the chick retina[J]. European Journal of Neuroscience, 1991, 3(6): 559-569.

Peichl L, González-Soriano J. Morphological types of horizontal cell in rodent retinae: a comparison of rat, mouse, gerbil, and guinea pig[J]. Visual neuroscience, 1994, 11(3): 501-517.

Pourcho R G, Goebel D J. Neuronal subpopulations in cat retina which accumulate the GABA agonist,(3H) muscimol: a combined Golgi and autoradiographic study[J]. Journal of Comparative Neurology, 1983, 219(1): 25-35.

Peltenburg L T, Murre C. Specific residues in the Pbx homeodomain differentially modulate the DNA-binding activity of Hox and Engrailed proteins[J]. Development, 1997, 124(5): 1089-1098.

Provenzano G, Clementi E, Genovesi S, et al. GH dysfunction in Engrailed-2 knockout mice, a model for autism spectrum disorders[J]. Frontiers in pediatrics, 2014b, 2: 92.

Provenzano G, Sgadò P, Genovesi S, et al. Hippocampal dysregulation of FMRP/mGluR5 signaling in engrailed-2 knockout mice: a model of autism spectrum disorders[J]. Neuroreport, 2015a, 26(18): 1101-1105.

Provenzano G, Pangrazzi L, Poli A, et al. Reduced phosphorylation of synapsin I in the hippocampus of Engrailed-2 knockout mice, a model for autism spectrum disorders[J]. Neuroscience, 2015b, 286: 122-130.

Provenzano G, Zunino G, Genovesi S, et al. Mutant mouse models of autism spectrum disorders[J]. Disease markers, 2012, 33(5): 225-239.

Panaitof S C. A songbird animal model for dissecting the genetic bases of autism spectrum disorder[J]. Disease markers, 2012, 33(5): 241-249.

Poché R A, Kwan K M, Raven M A, et al. Lim1 is essential for the correct laminar positioning of retinal horizontal cells[J]. Journal of Neuroscience,

2007, 27(51): 14099-14107.

Poole S J, Law M L, Kao F T, et al. Isolation and chromosomal localization of the human En-2 gene[J]. *Genomics*, 1989, 4(3): 225-231.

Ritvo E R, Freeman B J, Pingree C, et al. The UCLA-University of Utah epidemiological survey of autism: Prevalence[J]. *The American journal of psychiatry*, 1989, 146(2): 194.

Robertson, Caroline E., and Simon Baron-Cohen. Sensory perception in autism. *Nature Reviews Neuroscience* 18.11 (2017): 671.

Rogers S J, Hepburn S, Wehner E. Parent reports of sensory symptoms in toddlers with autism and those with other developmental disorders[J]. *Journal of autism and developmental disorders*, 2003, 33(6): 631-642.

Rosti RO, Sadek AA, Vaux KK, Gleeson JG. The genetic landscape of autism spectrum disorders. *Developmental Medicine & Child Neurology*. 2014 Jan 1;56(1):12-8.

Robert C, Pasquier L, Cohen D, Fradin M, Canitano R, Damaj L, Odent S, Tordjman S. Role of Genetics in the Etiology of Autistic Spectrum Disorder: Towards a Hierarchical Diagnostic Strategy. *International journal of molecular sciences*. 2017 Mar 12;18(3):618.

Reddy K S. Cytogenetic abnormalities and fragile-X syndrome in Autism Spectrum Disorder[J]. *BMC medical genetics*, 2005, 6(1): 3.

Romero-Munguía M Á. Mnesic imbalance and the neuroanatomy of autism spectrum disorders[M]//*Autism-A Neurodevelopmental Journey from Genes to Behaviour*. InTech, 2011.

Rodieck R W, Rodieck R W. *The first steps in seeing*[M]. Sunderland, MA: Sinauer Associates, 1998.

Rossignol R, Ranchon-Cole I, Pâris A, et al. Visual sensorial impairments in neurodevelopmental disorders: evidence for a retinal phenotype in Fragile X Syndrome[J]. *PloS one*, 2014, 9(8): e105996.

Smalley S L, Asarnow R F, Spence M A. Autism and genetics: a decade of research[J]. *Archives of general psychiatry*, 1988, 45(10): 953-961.

Suzuki H, Pinto L H. Response properties of horizontal cells in the isolated retina of wild-type and pearl mutant mice[J]. *Journal of Neuroscience*,

1986, 6(4): 1122-1128.

Singh SK, Eroglu C. Neuroligins provide molecular links between syndromic and nonsyndromic autism. *Sci. Signal.*. 2013 Jul 9;6(283):re4-.

Schaaf CP, Zoghbi HY. Solving the autism puzzle a few pieces at a time. *Neuron*. 2011 Jun 9;70(5):806-8.

Sztainberg Y, Zoghbi H Y. Lessons learned from studying syndromic autism spectrum disorders. *Nature neuroscience*. 2016 Nov;19(11):1408.

Sgaier S K, Lao Z, Villanueva M P, et al. Genetic subdivision of the tectum and cerebellum into functionally related regions based on differential sensitivity to engrailed proteins[J]. *Development*, 2007, 134(12): 2325-2335.

Sgadò P, Genovesi S, Kalinovsky A, et al. Loss of GABAergic neurons in the hippocampus and cerebral cortex of Engrailed-2 null mutant mice: implications for autism spectrum disorders[J]. *Experimental neurology*, 2013, 247: 496-505.

Sgadò P, Dunleavy M, Genovesi S, et al. The role of GABAergic system in neurodevelopmental disorders: a focus on autism and epilepsy[J]. *International journal of physiology, pathophysiology and pharmacology*, 2011, 3(3): 223.

Sonntag S, Dedek K, Dorgau B, et al. Ablation of retinal horizontal cells from adult mice leads to rod degeneration and remodeling in the outer retina[J]. *Journal of Neuroscience*, 2012, 32(31): 10713-10724.

Sudarov A, Joyner A L. Cerebellum morphogenesis: the foliation pattern is orchestrated by multi-cellular anchoring centers[J]. *Neural development*, 2007, 2(1): 26.

Tolkunova E N, Fujioka M, Kobayashi M, et al. Two distinct types of repression domain in engrailed: one interacts with the groucho corepressor and is preferentially active on integrated target genes[J]. *Molecular and cellular biology*, 1998, 18(5): 2804-2814.

Tripathi P P, Sgado P, Scali M, et al. Increased susceptibility to kainic acid-induced seizures in Engrailed-2 knockout mice[J]. *Neuroscience*, 2009, 159(2): 842-849.

Taylor W R, Vaney D I. New directions in retinal research[J]. *Trends in*

- neurosciences, 2003, 26(7): 379-385.
- Thoreson W.B. The Vertebrate Retina. In: Gendelman H.E., Ikezu T. (eds) Neuroimmune Pharmacology. 2008 , Springer, Boston, MA
- Thoreson W B, Mangel S C. Lateral interactions in the outer retina[J]. Progress in retinal and eye research, 2012, 31(5): 407-441.
- Vlamings P H J M, Jonkman L M, van Daalen E, et al. Basic abnormalities in visual processing affect face processing at an early age in autism spectrum disorder[J]. Biological psychiatry, 2010, 68(12): 1107-1113.
- Vorstman JA, Staal WG, van Daalen E, van Engeland H, Hochstenbach PF, Franke L. Identification of novel autism candidate regions through analysis of reported cytogenetic abnormalities associated with autism. Mol Psychiatry 2006;11:1, 18–28.
- Veenstra-Vanderweele, J., Christian, S. L., Cook, E. H. (2004). Autism as a paradigmatic complex genetic disorder. Annual Review of Genomics and Human Genetics, 5, 379–405.
- Van Dijk M A, Murre C. extradenticle raises the DNA binding specificity of homeotic selector gene products[J]. Cell, 1994, 78(4): 617-624.
- Wing L, Yeates S R, Brierley L M, et al. The prevalence of early childhood autism: comparison of administrative and epidemiological studies[J]. Psychological medicine, 1976, 6(1): 89-100.
- Wässle H, Peichl L, Airaksinen M S, et al. Calcium-binding proteins in the retina of a calbindin-null mutant mouse[J]. Cell and tissue research, 1998, 292(2): 211-218.
- Williams D. Nobody nowhere: The remarkable autobiography of an autistic girl[M]. Jessica Kingsley Publishers, 2009.
- Watling R L, Deitz J, White O. Comparison of Sensory Profile scores of young children with and without autism spectrum disorders[J]. American Journal of Occupational Therapy, 2001, 55(4): 416-423.
- Wulle I, Schnitzer J. Distribution and morphology of tyrosine hydroxylase-immunoreactive neurons in the developing mouse retina. Developmental Brain Research. 1989 Jul 1;48(1):59-72.
- Wilson S L, Kalinovsky A, Orvis GD, et al. Spatially restricted and

- developmentally dynamic expression of engrailed genes in multiple cerebellar cell types [J]. *The Cerebellum*, 2011, 10(3): 356-372.
- Wizenmann A, Stettler O, Moya K L. Engrailed homeoproteins in visual system development[J]. *Cellular and molecular life sciences*, 2015, 72(8): 1433-1445.
- Wizenmann A, Brunet I, Lam J S Y, et al. Extracellular Engrailed participates in the topographic guidance of retinal axons in vivo[J]. *Neuron*, 2009, 64(3): 355-366.
- Wang Y, Zhong H, Wang C, et al. Maternal exposure to the water soluble fraction of crude oil, lead and their mixture induces autism-like behavioral deficits in zebrafish (*Danio rerio*) larvae[J]. *Ecotoxicology and environmental safety*, 2016, 134: 23-30.
- Wässle H. Parallel processing in the mammalian retina[J]. *Nature Reviews Neuroscience*, 2004, 5(10): 747.
- Xu Y, Sulaiman P, Feddersen R M, et al. Retinal ON bipolar cells express a new PCP2 splice variant that accelerates the light response[J]. *Journal of Neuroscience*, 2008, 28(36): 8873-8884.
- Young R W. Cell differentiation in the retina of the mouse[J]. *The Anatomical Record*, 1985, 212(2): 199-205.
- Yabut O, Renfro A, Niu S, et al. Abnormal laminar position and dendrite development of interneurons in the reeler forebrain[J]. *Brain research*, 2007, 1140: 75-83.
- Yip J, Soghomonian J J, Blatt G J. Increased GAD67 mRNA expression in cerebellar interneurons in autism: implications for Purkinje cell dysfunction[J]. *Journal of neuroscience research*, 2008, 86(3): 525-530.
- Zoghbi H Y, Bear M F. Synaptic dysfunction in neurodevelopmental disorders associated with autism and intellectual disabilities[J]. *Cold Spring Harbor perspectives in biology*, 2012, 4(3): a009886.
- Zhang X M, Yang X J. Regulation of retinal ganglion cell production by Sonic hedgehog[J]. *Development*, 2001, 128(6): 943-957.
- Zhang T, Cao LH, Kumar S, Enemchukwu NO, Zhang N, Lambert A, Zhao X, Jones A, Wang S, Dennis EM, Fnu A. Dimerization of visual pigments in

vivo. Proceedings of the National Academy of Sciences. 2016 Aug 9;113(32):9093-8.

ACKNOWLEDGEMENTS

Firstly, I would like to express my sincere gratitude to my tutor Prof. Simona Casarosa for her patient and effective guidance and continuous support for my PhD study and research. Her strict and professional training has dramatically improved my ability to think precisely and aggressively. More importantly, her rigorous attitude to work and science deserves my respect and I think it will also benefit me a lot for my future career.

I'm also extremely grateful to my advisor Dr. Andrea Messina. During the past three years, he always stands with me when I have doubts and problems for my project, and gives me numerous useful suggestions for my project. I also want to specially thank Prof. Yuri Bozzi for his continuous kind support for my PhD project. Besides, I want to thank my present and previous fellow labmates, Giovanni, Alessandra, Mariaelena, Francesca, Bartolomeo, Angela for the wonderful period working together with them and their kind help for my life in Italy. I am also grateful to our collaborator, Prof. Claudia Gargini and her lab members from University of Pisa for their wonderful work supporting my PhD project.

I would like to express a special thank to my family, in particular, my parents, my beloved wife, Yingfen, and my lovely daughter, Yiya. Thank you for their gorgeous support and constant companion to encourage me to pass through

every tough period during my PhD.

I would like to thank my friends, Eyemen, Rama, Preet for their gorgeous help and the relaxed coffee break during my PhD. I also want to express appreciation to the colleagues in Cibio for their technical support for my project, in particular, Giogina, Sara, Michela from the Advanced Imaging Core Facility (AICF), Marta from the animal facility, Michael from the High Troughput Screening (HTS) facility.

I also want to thank China Scholarship Council (CSC) to provide me the scholarship to support my PhD study in Italy.

Finally, I would like to express my appreciation to Italy for giving me and my family the amazing landscape and culture experience, as well as warm and unforgettable memory during the past three years. Grazie!